

## ***Supplementary Materials for ‘Unsupervised Sensitivity Prior Generation with Diffusion Model for EIT Image Reconstruction’***

**Abstract-** In these supplementary materials, we provide more information including the homogeneous/inhomogeneous sensitivity maps and correspond analysis, the detailed descriptions of training datasets. Moreover, for sufficiently illustrating the reconstruction performances between our SPfusion and related comparison methods, the extensive experiment results are given.

**Index terms:** EIT, inverse problem, sensitivity prior, diffusion model, dual-domain Transformer.

### I . Sensitivity prior:

The homogeneous sensitivity is usually utilized in the conventional model-based reconstruction algorithms as we can assume a reference state for calculating the Jacobian matrix according to the  $S'(\mathbf{x}_0) = \frac{\mathbf{U} - \mathbf{U}_0}{\mathbf{x} - \mathbf{x}_0} = \frac{\partial \mathbf{U}}{\partial \mathbf{x}} \Big|_{\mathbf{x}=\mathbf{x}_0}$ . The element in this homogeneous sensitivity matrix is obtained according to the Geselowitz sensitivity theorem, which is expressed as

$$S_{i,j} = - \int_{e_N} \frac{\nabla \varphi(I^i)}{I^i} \cdot \frac{\nabla \varphi(I^j)}{I^j} d\mathbf{e}_N \quad (1)$$

However, this linear approximation idea will loss the high-order nonlinear terms that contain the structural features and electrical parameters. With this insight, we give the visualizations of the homogeneous sensitivity maps and the inhomogeneous sensitivity maps of three cases in Figure 7, which could show the differences between the homogeneous and inhomogeneous sensitivity distributions.

Considering the sensitivity prior is expressed as the three-order tensor with the size of  $M \times N \times N$ ,  $M$  indicates the measurement number and  $N$  is the resolution of sensitivity map, we show these maps with two-dimensional figures of each slice. In this work, the  $M$  is 208 expressing the measured voltages based on the adjacent current excitation and adjacent voltage measurement protocol, the  $N$  is set as 256 expressing the grid of inverse problem. Further, we also give the three-dimensional maps of sensitivity distributions under different excitation-measurement sequences.

The Figures S1 to S12 are shown as follows, where the S1 and S4 figures correspond to the case 1 in Figure 7, S5 and S8 figures correspond to the case 2 in Figure 7, and S9 and S12 figures correspond to the case 3 in Figure 7.

### II . Datasets:

The observation area is set a circular shape with the diameter of 0.19 m, and there are 16 electrodes uniformly attached on the outside boundary of the domain. The protocol of data acquisition is ‘adjacent current excitation-adjacent voltage measurement’, where the current is utilized with the amplitude of 4.5 mA and the frequency of 50kHz. The NaCl solution with 0.06 S/m is set up as background in the homogeneous field. The forward problem of EIT is solved by finite elements method (FEM), the observation domain is discretized into a triangular mesh and then solved. For the 16-electrode EIT measurement model, a total of 208 voltages are obtained for all electrodes excitation-measurement at one time. In order to avoid the problem of ‘inverse crime’, different discrete meshes are used to characterize the conductivity distribution in the domain. The observation domain is divided using square grids into  $256 \times 256$  pixels to adequately represent information about inclusions with complex boundary shapes.

**(1) Multi-phase inclusion distributions:** The inclusions with multi-phase distributions with the conductivity in the range of  $10^{-6}$ - $10^6$  S/m. The radius is set in the range of 0.02-0.08m, the number of inclusions is set as from 1 to 4. These inclusions do not intersect each other. A total of 52,430 (containing 42,430 circle inclusions and 10,000 shaped inclusions) simulation samples are obtained. The training, validation and test samples are set to be 80%, 10% and 10% of the total database respectively.

**(2) Healthy/injured lung-phantoms:** The structured information of the human chest is obtained according to the CT image, and the process of constructing simulation models is described in the literature. The conductivities of healthy organs are set as: fat with 0.30 S/m, heart with 0.50 S/m, aorta with 0.60 S/m, spine with 0.09 S/m, and the inflated lung with 0.15 S/m. The lung injury is simulated by randomly removing a portion of the lungs and replacing the missing portion with the other medium, where the conductivity of the injured lungs ranges from 0.165 to 0.285 S/m. For augmenting the simulation data, the Gaussian white noise is added to the measurements with a signal-to-noise ratio (SNR) of 65 dB. Finally, the number of simulated lung phantoms is 9,100 for training and 1,000 for testing, respectively.

Each sample in the database contains three information of homogeneous sensitivity  $\mathbf{S}^h$ , inhomogeneous sensitivity  $\mathbf{S}^i$ , and the differential measurement voltages  $\mathbf{U}$ . Here, the  $\mathbf{S}^h$  is obtained without inclusions in the observation domain,  $\mathbf{S}^i$  is obtained with inclusions in the observation domain, and  $\mathbf{U}$  is difference between the vector of boundary measurement with inclusions and without inclusions.

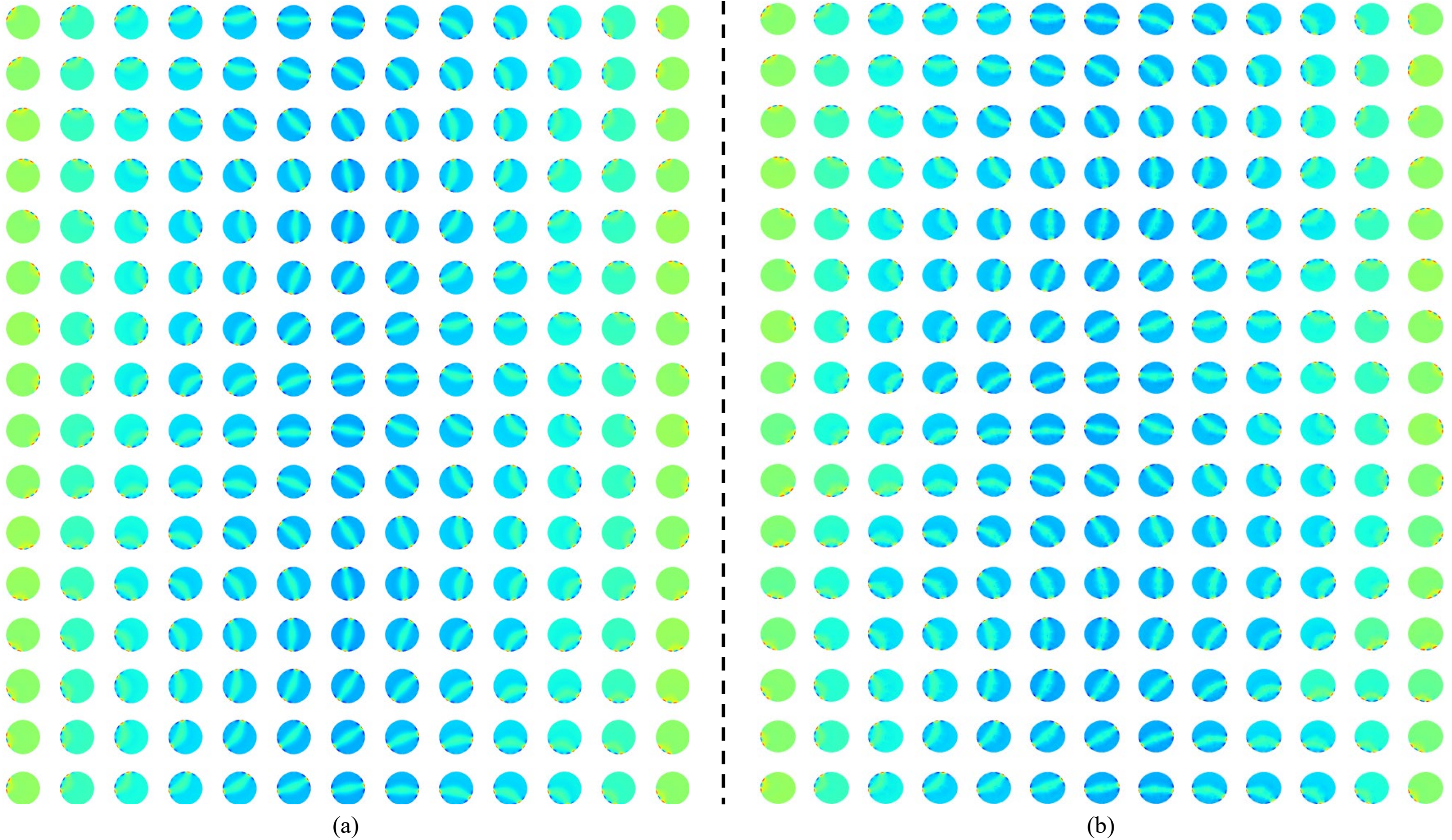


Fig. S1 The visualizations of sensitivity maps of In-Distribution data (multi-phase inclusions). Based on the 16-electrode EIT system with adjacent current excitation and adjacent voltage measurement, there are 208 measurements acquired for expressing one completed cross-section. (a) The maps of homogeneous sensitivity distributions. (b) The maps of inhomogeneous sensitivity distributions. The zoom figures of representative distributions are given in Fig. S2.

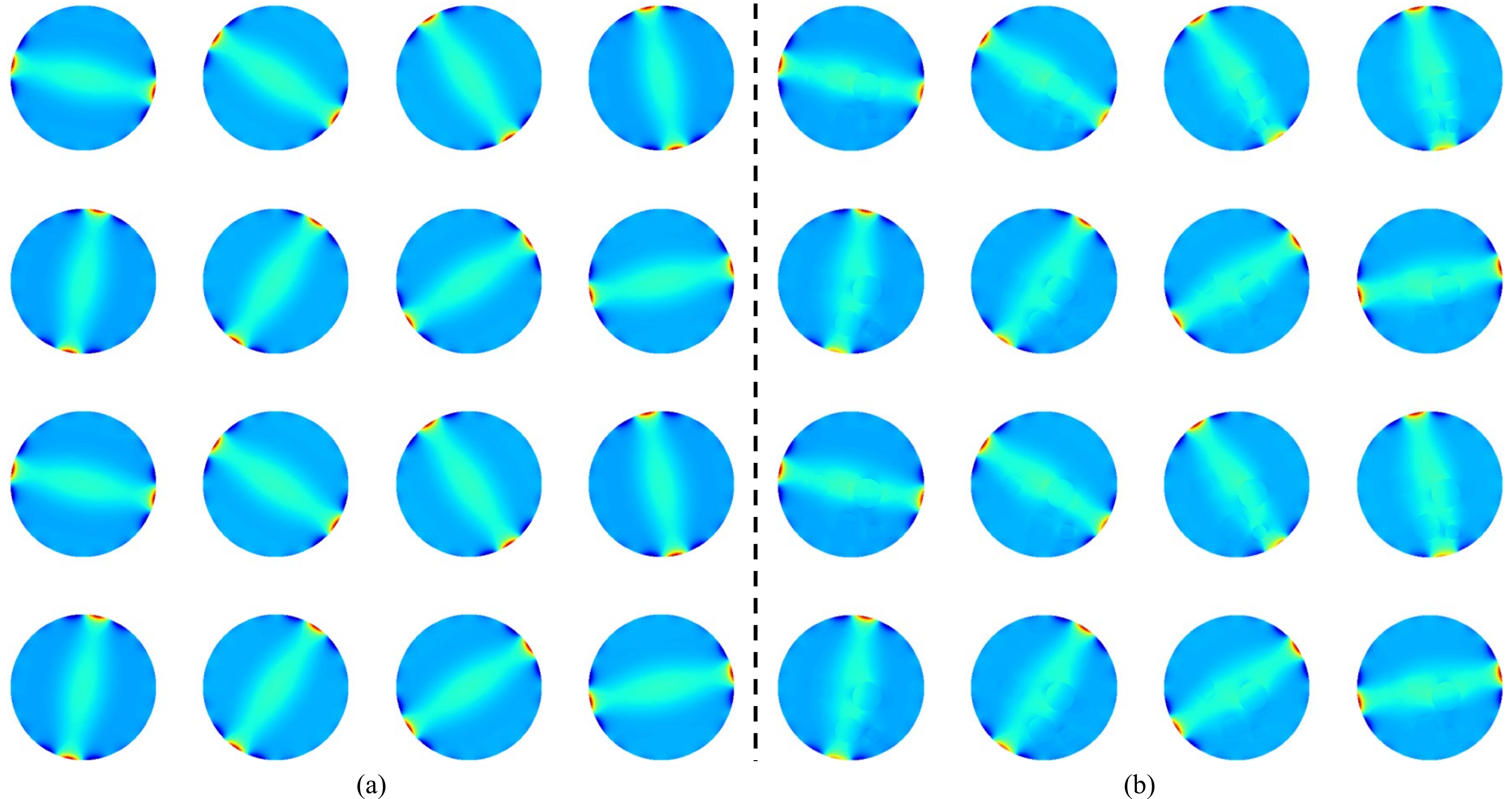


Fig. S2 The visualizations of sensitivity maps of In-Distribution data (multi-phase inclusions). (a) The maps of homogeneous sensitivity distributions. (b) The maps of inhomogeneous sensitivity distributions. For choosing the representative results, the diagonal sensitivity distributions are considered, which could clearly show the sensitivity information in the ‘center’ domain. According to the (a) and (b), the clear differences, especially the structural information, are highlighted for introducing the rich priors in the inhomogeneous sensitivity distributions.

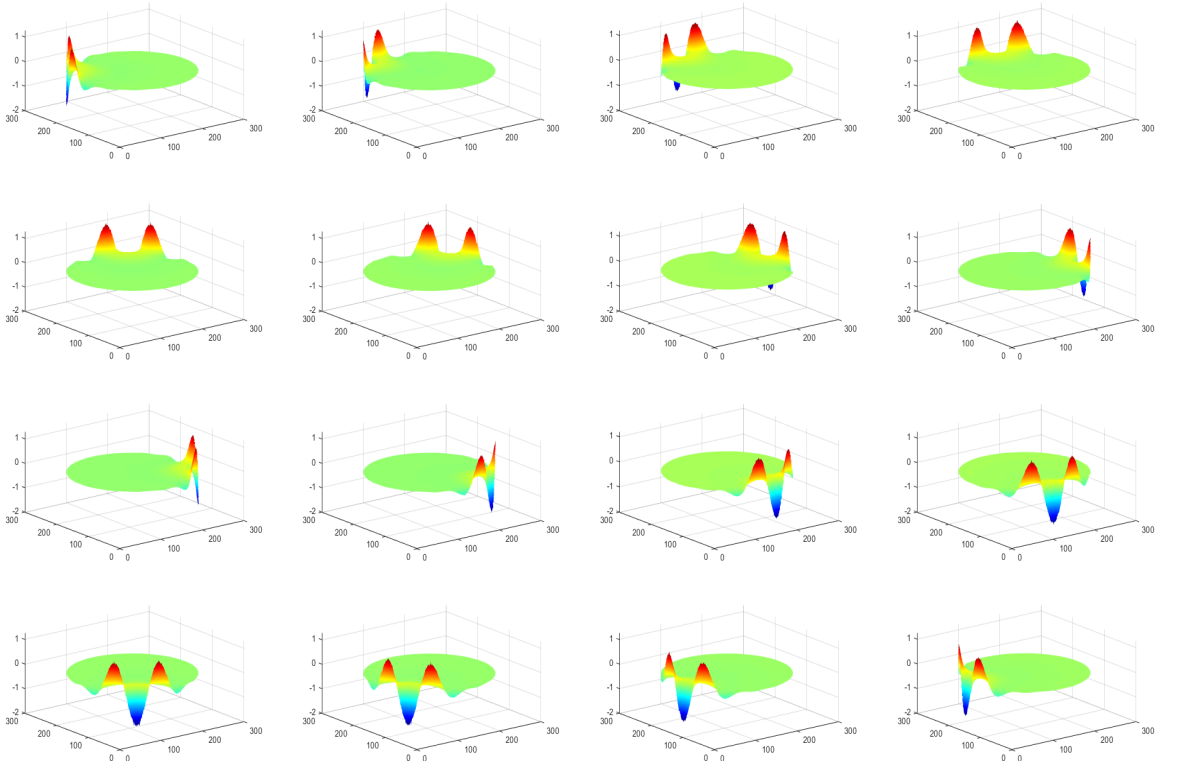


Fig. S3 The three dimension visualizations of homogeneous sensitivity maps of In-Distribution datasets with multi-phase inclusions imaging tasks. In this figure, the labels of x-axis and y-axis are marked to illustrate the spatial resolution, and z-axis give the sensitivity values. Based on the 16-electrode EIT system with adjacent current excitation and adjacent voltage measurement, there are 208 measurements acquired for expressing one completed cross-section. We select the 1, 14, 27, 40, 53, 65, 78, 91, 104, 117, 130, 143, 156, 169, 182, 195 excitation-measurement state to show the sensitivity distributions.

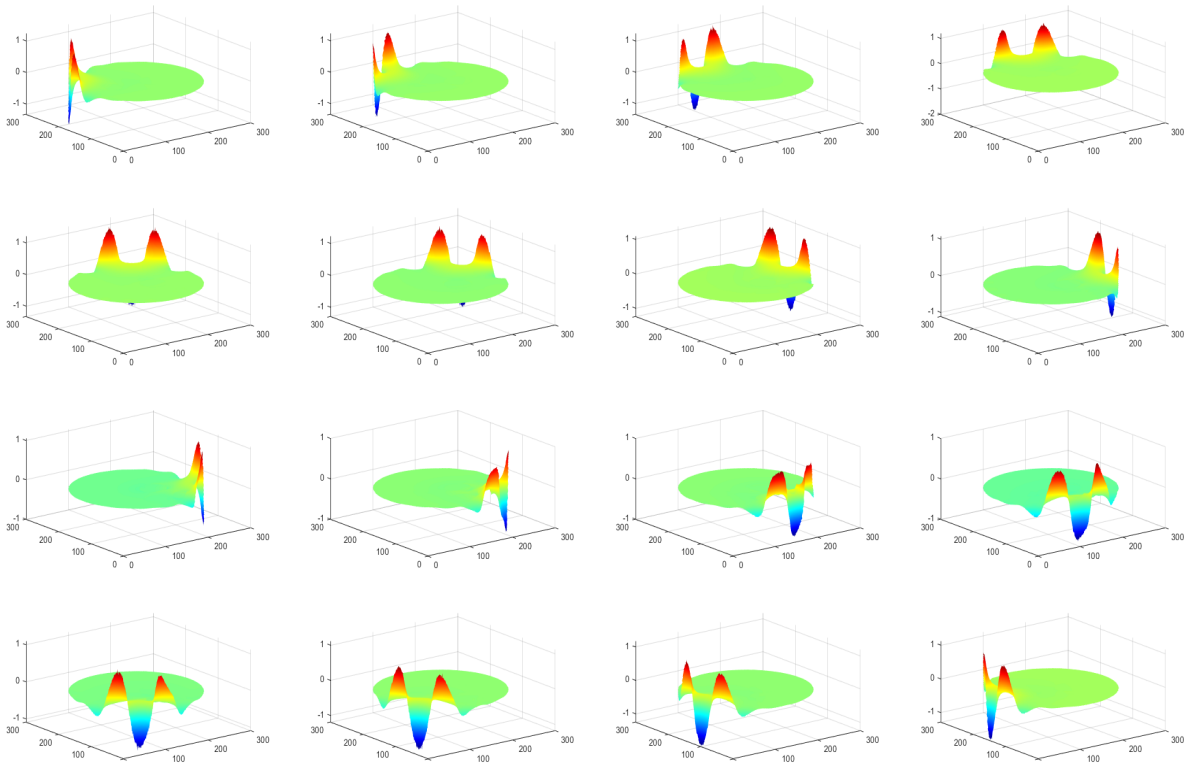


Fig. S4 The visualizations of inhomogeneous sensitivity maps of In-Distribution data (Case 1 in Figure 8) with multi-phase inclusions imaging tasks. In this figure, the labels of x-axis and y-axis are marked to illustrate the spatial resolution, and z-axis give the sensitivity values. Based on the 16-electrode EIT system with adjacent current excitation and adjacent voltage measurement, there are 208 measurements acquired for expressing one completed cross-section. We select the 1, 14, 27, 40, 53, 65, 78, 91, 104, 117, 130, 143, 156, 169, 182, 195 excitation-measurement state to show the sensitivity distributions.

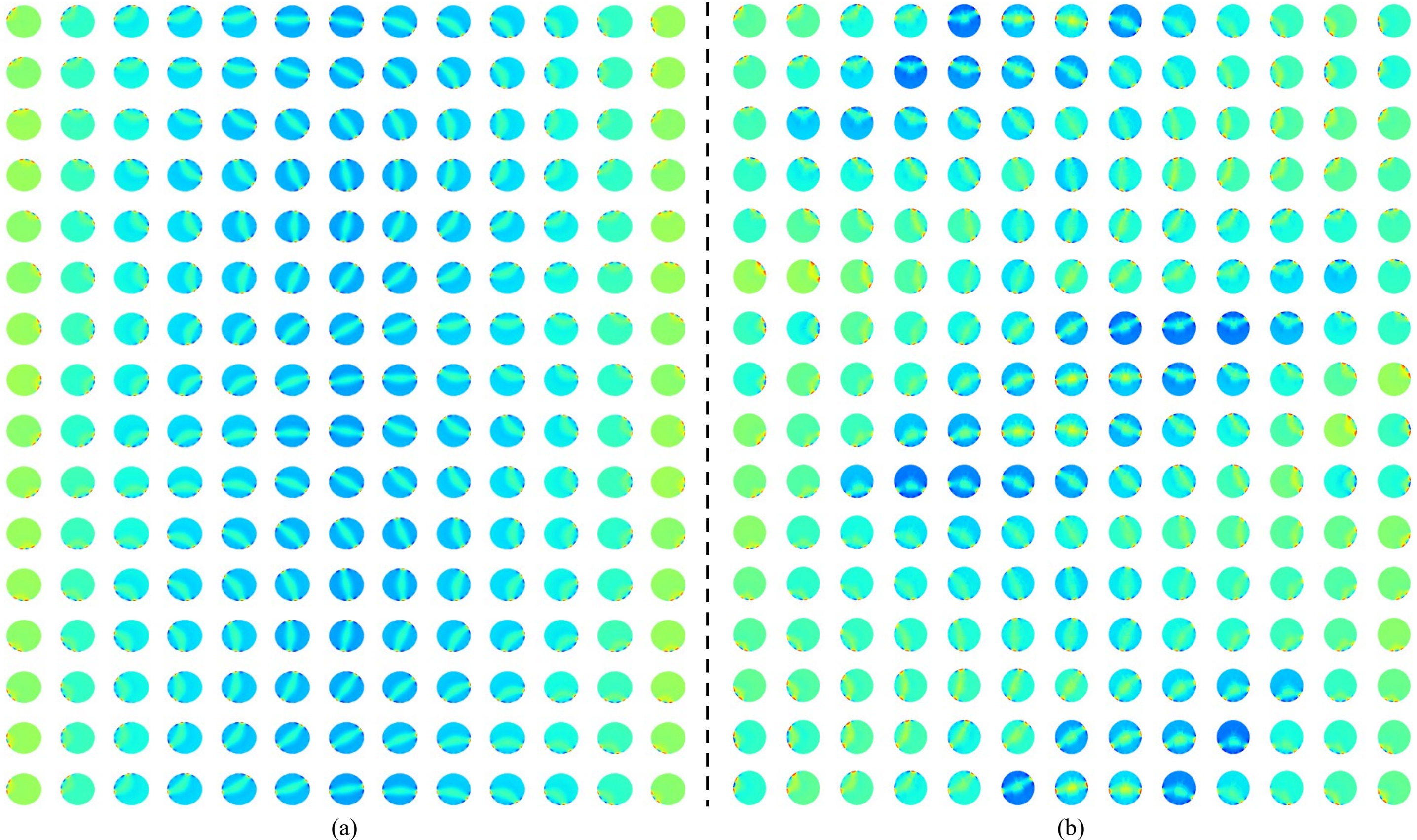


Fig. S5 The visualizations of sensitivity maps of In-Distribution data (lung-shaped phantoms). Based on the 16-electrode EIT system with adjacent current excitation and adjacent voltage measurement, there are 208 measurements acquired for expressing one completed cross-section. (a) The maps of homogeneous sensitivity distributions. (b) The maps of inhomogeneous sensitivity distributions. The zoom figures of representative distributions are given in Fig. S6.

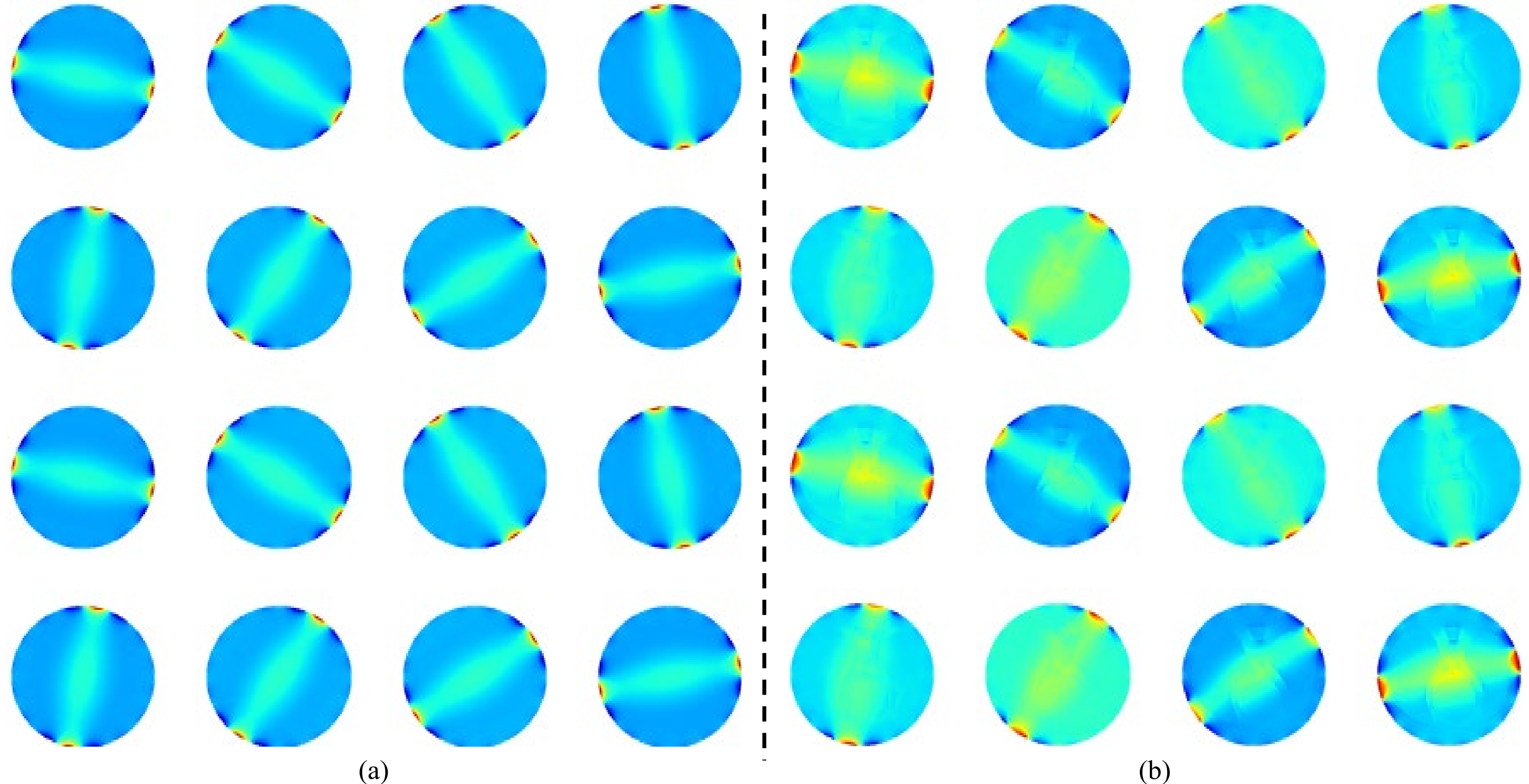


Fig. S6 The visualizations of sensitivity maps of In-Distribution data (multi-phase inclusions). (a) The maps of homogeneous sensitivity distributions. (b) The maps of inhomogeneous sensitivity distributions. For choosing the representative results, the diagonal sensitivity distributions are considered, which could clearly show the sensitivity information in the ‘center’ domain. According to the (a) and (b), the clear differences, especially the structural information, are highlighted for introducing the rich priors in the inhomogeneous sensitivity distributions.

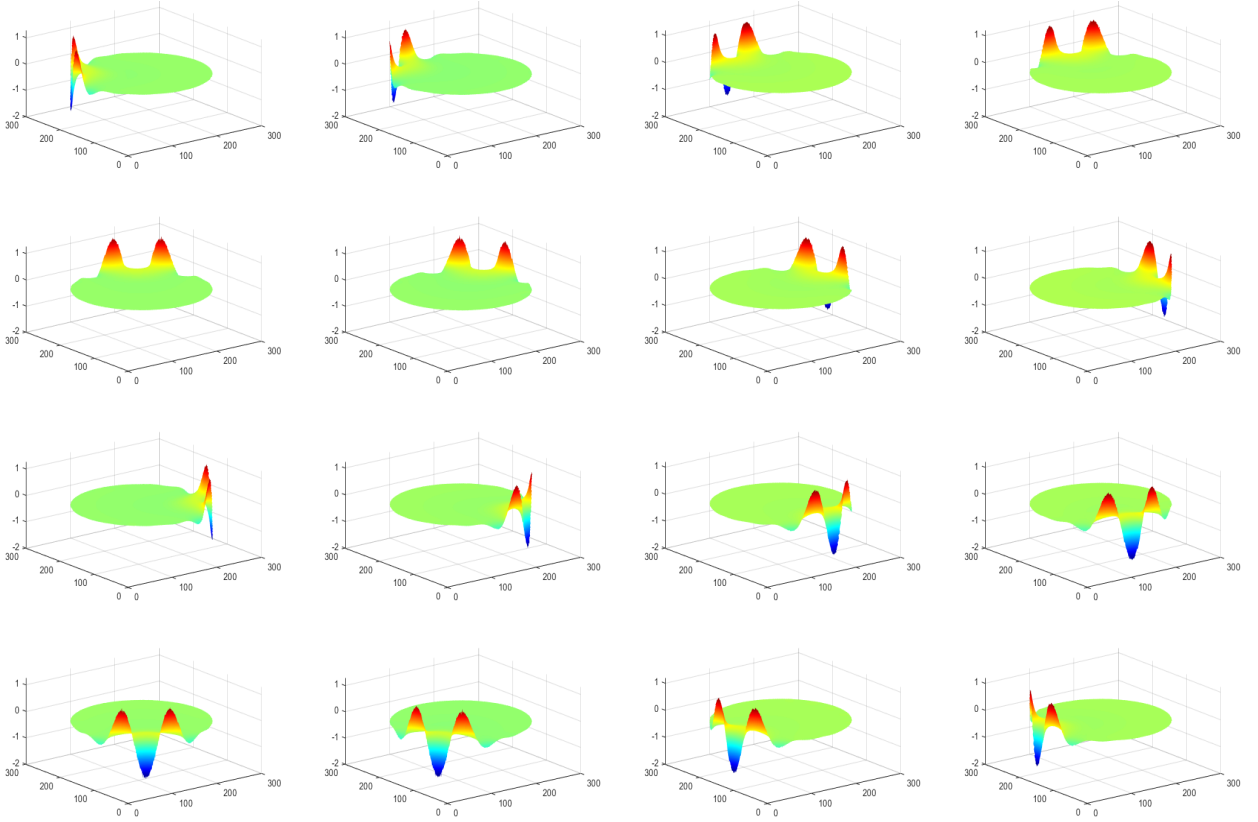


Fig. S7 The three dimension visualizations of homogeneous sensitivity maps of In-Distribution datasets with lung-shaped phantoms imaging tasks. In this figure, the labels of x-axis and y-axis are marked to illustrate the spatial resolution, and z-axis give the sensitivity values. Based on the 16-electrode EIT system with adjacent current excitation and adjacent voltage measurement, there are 208 measurements acquired for expressing one completed cross-section. We select the 1, 14, 27, 40, 53, 65, 78, 91, 104, 117, 130, 143, 156, 169, 182, 195 excitation-measurement state to show the sensitivity distributions.

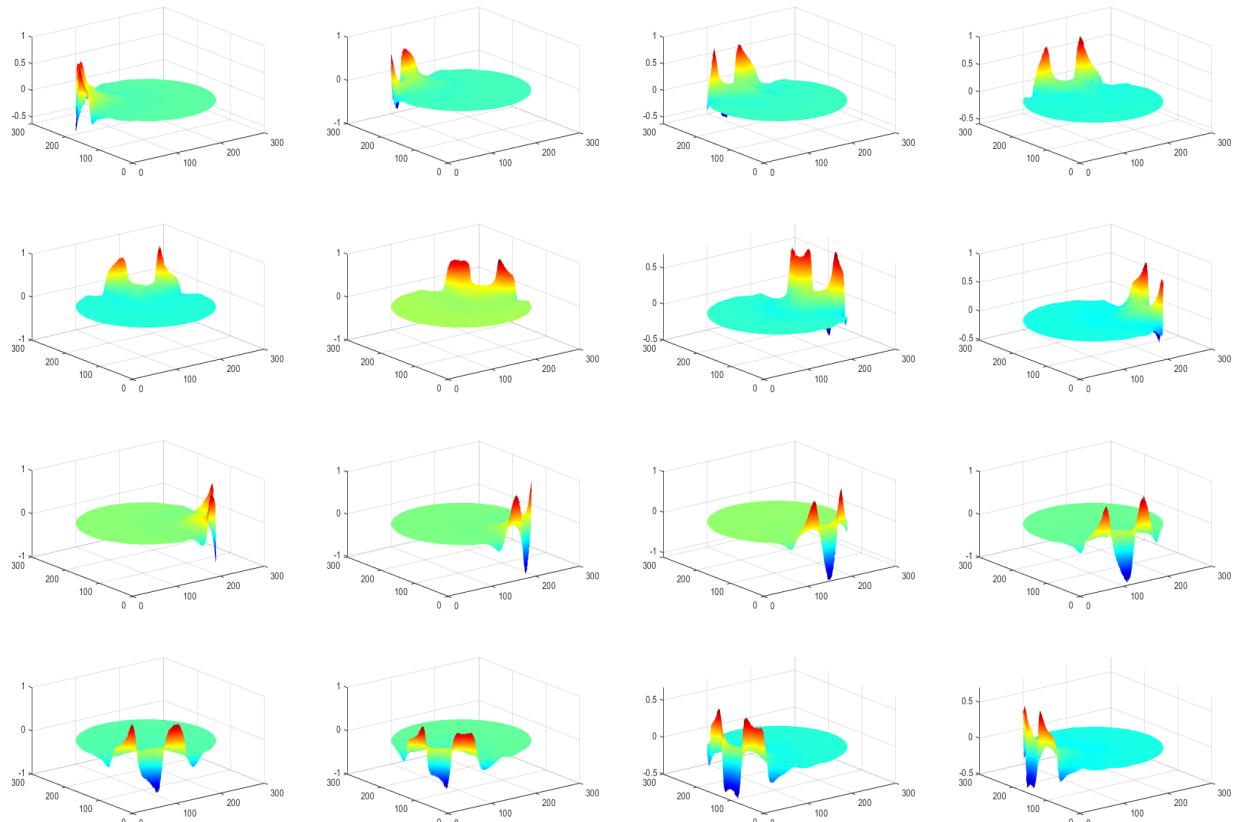


Fig. S8 The visualizations of inhomogeneous sensitivity maps of In-Distribution data (Case 2 in Figure 8) with lung-shaped phantoms imaging tasks. In this figure, the labels of x-axis and y-axis are marked to illustrate the spatial resolution, and z-axis give the sensitivity values. Based on the 16-electrode EIT system with adjacent current excitation and adjacent voltage measurement, there are 208 measurements acquired for expressing one completed cross-section. We select the 1, 14, 27, 40, 53, 65, 78, 91, 104, 117, 130, 143, 156, 169, 182, 195 excitation-measurement state to show the sensitivity distributions.

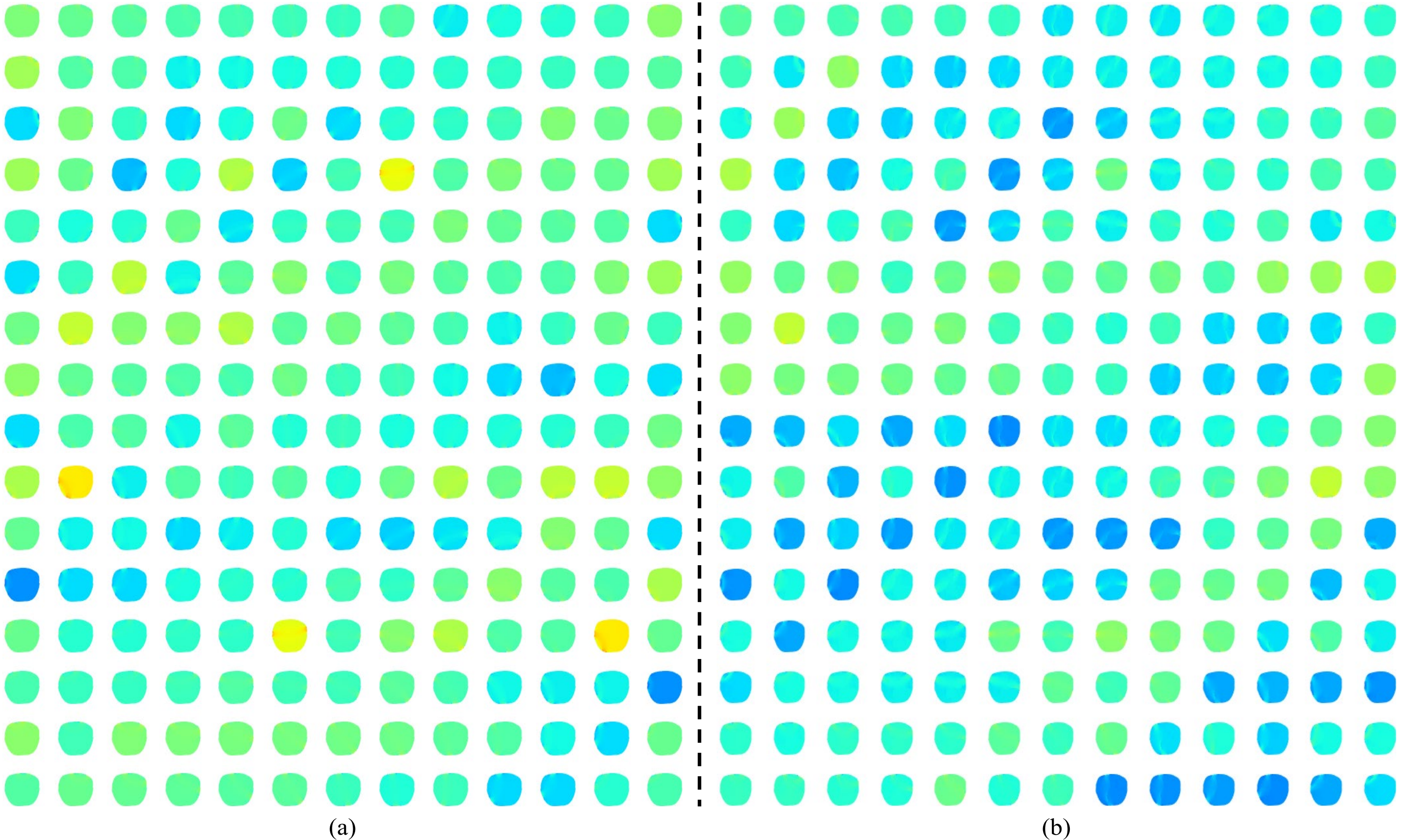


Fig. S9 The visualizations of sensitivity maps of Out-of-Distribution data (chest-shaped observation domain). Based on the 16-electrode EIT system with adjacent current excitation and adjacent voltage measurement, there are 208 measurements acquired for expressing one completed cross-section. (a) The maps of homogeneous sensitivity distributions. (b) The maps of inhomogeneous sensitivity distributions. The zoom figures of representative distributions are given in Fig. S10.

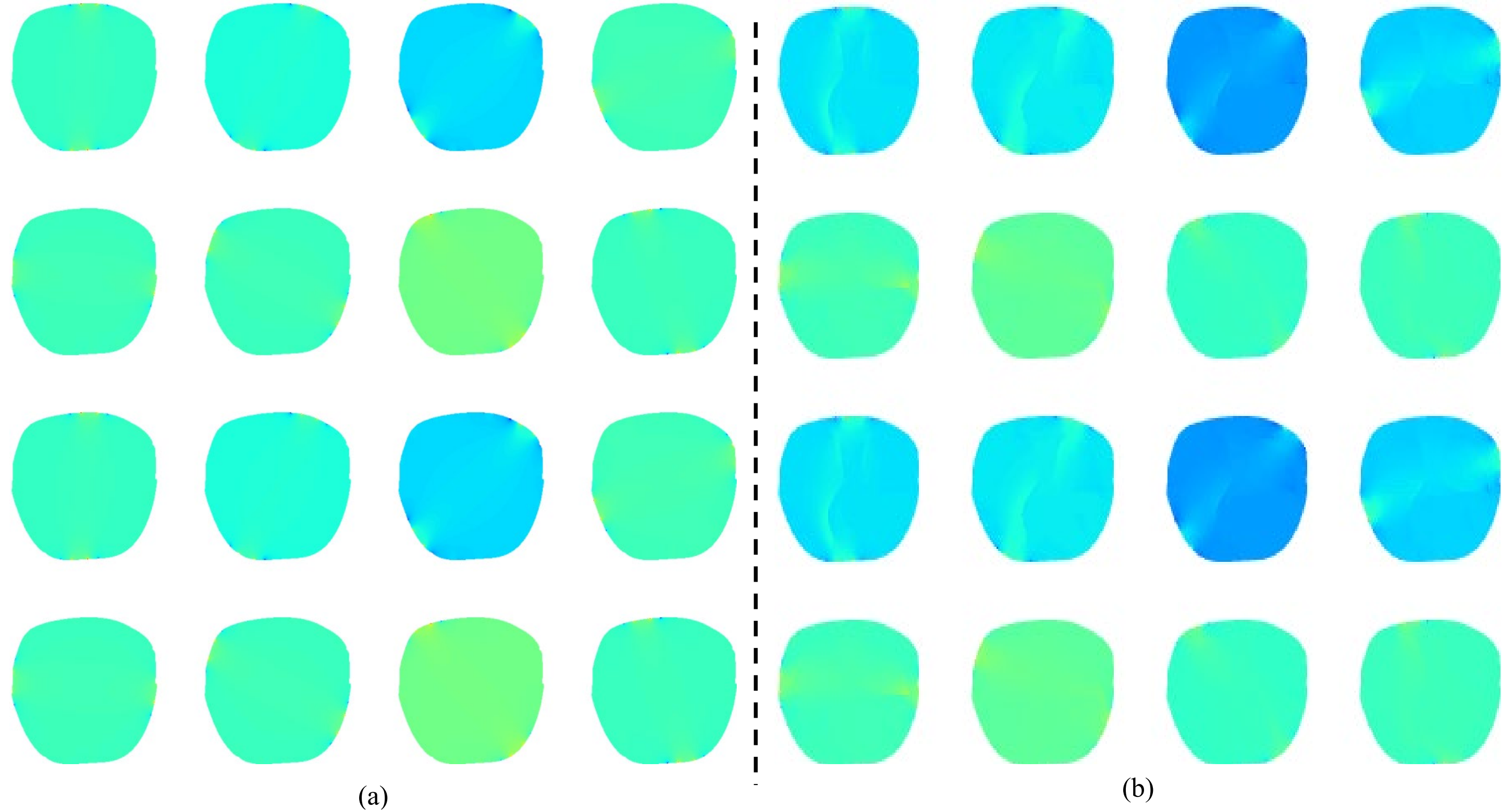


Fig. S10 The visualizations of sensitivity maps of Out-of-Distribution data (chest-shaped observation domain). (a) The maps of homogeneous sensitivity distributions. (b) The maps of inhomogeneous sensitivity distributions. For choosing the representative results, the diagonal sensitivity distributions are considered, which could clearly show the sensitivity information in the ‘center’ domain. According to the (a) and (b), the clear differences, especially the structural information, are highlighted for introducing the rich priors in the inhomogeneous sensitivity distributions.

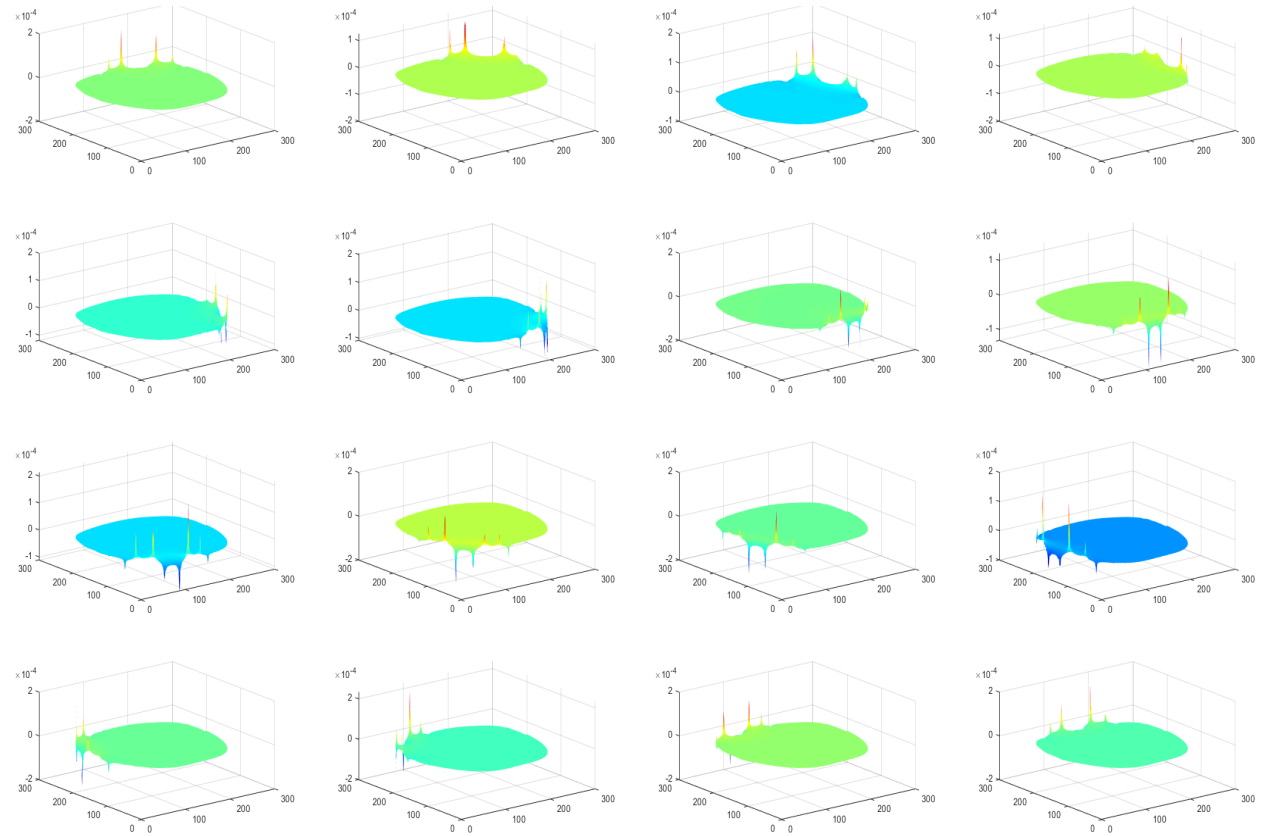


Fig. S11 The three dimension visualizations of homogeneous sensitivity maps of Out-of-Distribution datasets with chest-shaped domain imaging tasks. In this figure, the labels of x-axis and y-axis are marked to illustrate the spatial resolution, and z-axis give the sensitivity values. Based on the 16-electrode EIT system with adjacent current excitation and adjacent voltage measurement, there are 208 measurements acquired for expressing one completed cross-section. We select the 1, 14, 27, 40, 53, 65, 78, 91, 104, 117, 130, 143, 156, 169, 182, 195 excitation-measurement state to show the sensitivity distributions.

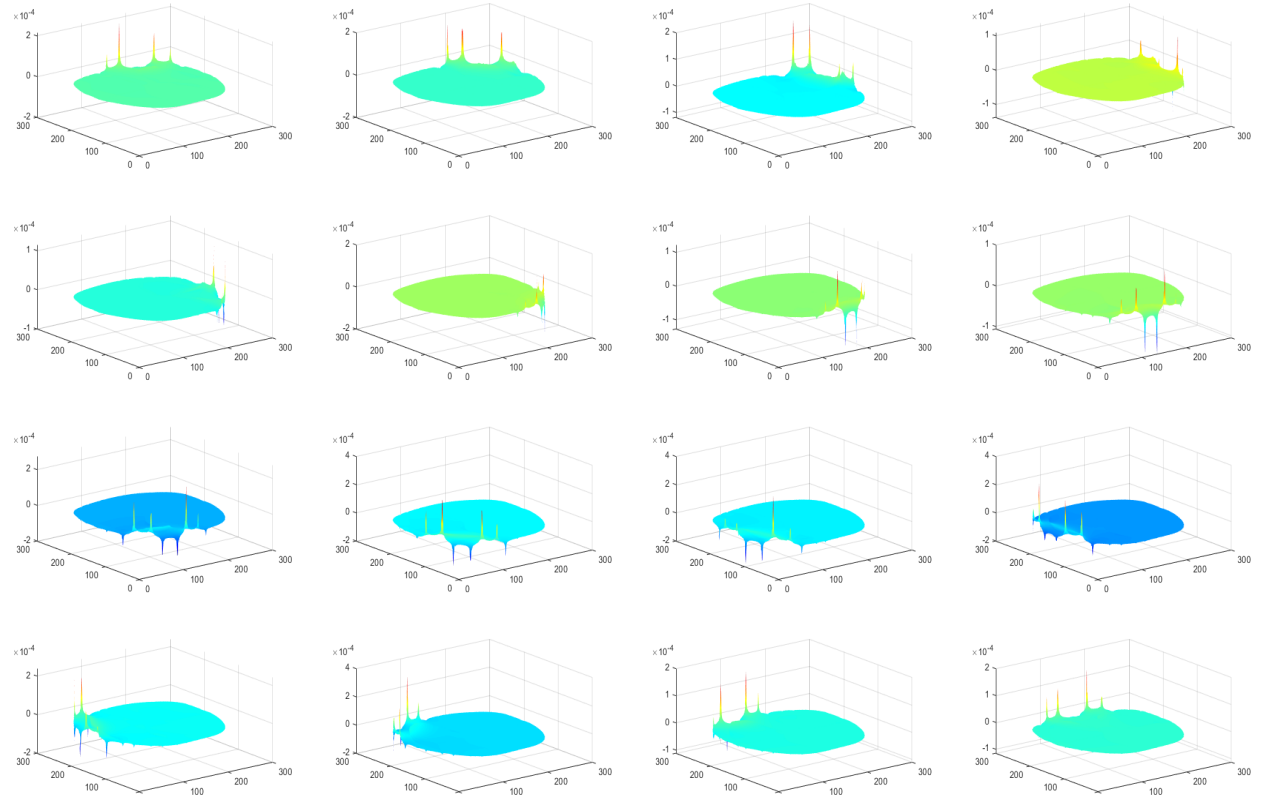


Fig. S12 The visualizations of inhomogeneous sensitivity maps of Out-of-Distribution data (Case 3 in Figure 8) with chest-shaped domain imaging tasks. In this figure, the labels of x-axis and y-axis are marked to illustrate the spatial resolution, and z-axis give the sensitivity values. Based on the 16-electrode EIT system with adjacent current excitation and adjacent voltage measurement, there are 208 measurements acquired for expressing one completed cross-section. We select the 1, 14, 27, 40, 53, 65, 78, 91, 104, 117, 130, 143, 156, 169, 182, 195 excitation-measurement state to show the sensitivity distributions.

### III. Extensive experimental results:

In this section, we will give more image reconstruction results based on the In-Distribution datasets and Out-of-Distribution datasets.

#### A. Results of In-Distribution data:

In the In-Distribution experiments, the inclusions distributions of the training and testing datasets are the same, and the shape of observation area is the circular. The results are shown in Figures S13 to S16. In each case, the first column is the ground truth or experimental settings, the second to fifth columns are the results based on the supervised-based image-domain reconstruction methods (DHU-Net [9], FISTA-Net [10], PDCISTA-Net [11], SWISTA-Net [26]), the sixth to ninth columns give the results of the unsupervised-based image-domain reconstruction methods (DeepEIT [27], DiffusionEIT [18], ConditionDDPM [20] and CD-EIT [19]), the tenth to twelfth columns give the results of the unsupervised-based image-domain reconstruction methods (CGAN [28], DDPM [24] and proposed SPfusion, these results are reconstructed by FISTA-Net).

#### B. Results of Out-of-Distribution data:

In this section, the chest-shaped areas experiments are conducted to evaluate the influence of boundary conditions on the sensitivity prior. The results are shown in Figures S17 to S19. In each case, the first column is the ground truth or experimental settings, the second to fifth columns are the results based on the supervised-based image-domain reconstruction methods (DHU-Net [9], FISTA-Net [10], PDCISTA-Net [11], SWISTA-Net [26]), the sixth to ninth columns give the results of the unsupervised-based image-domain reconstruction methods (DeepEIT [27], DiffusionEIT [18], ConditionDDPM [20] and CD-EIT [19]), the tenth to twelfth columns give the results of the unsupervised-based image-domain reconstruction methods (CGAN [28], DDPM [24] and proposed SPfusion, these results are reconstructed by FISTA-Net).

#### C. Quantitative metrics and analysis:

In this section, the quantitative metrics (RMSE, PSNR, and SSIM) of real-world test cases are given in Tables SI (the results of Figure S15), SII (the results of Figure S16), as well as Tables SIII to SV (the results of Figures S17 to S19). The results of Tables SI and SII are the metrics of in-distribution test data, and Tables SIII to SV are the metrics of out-of-distribution test data.

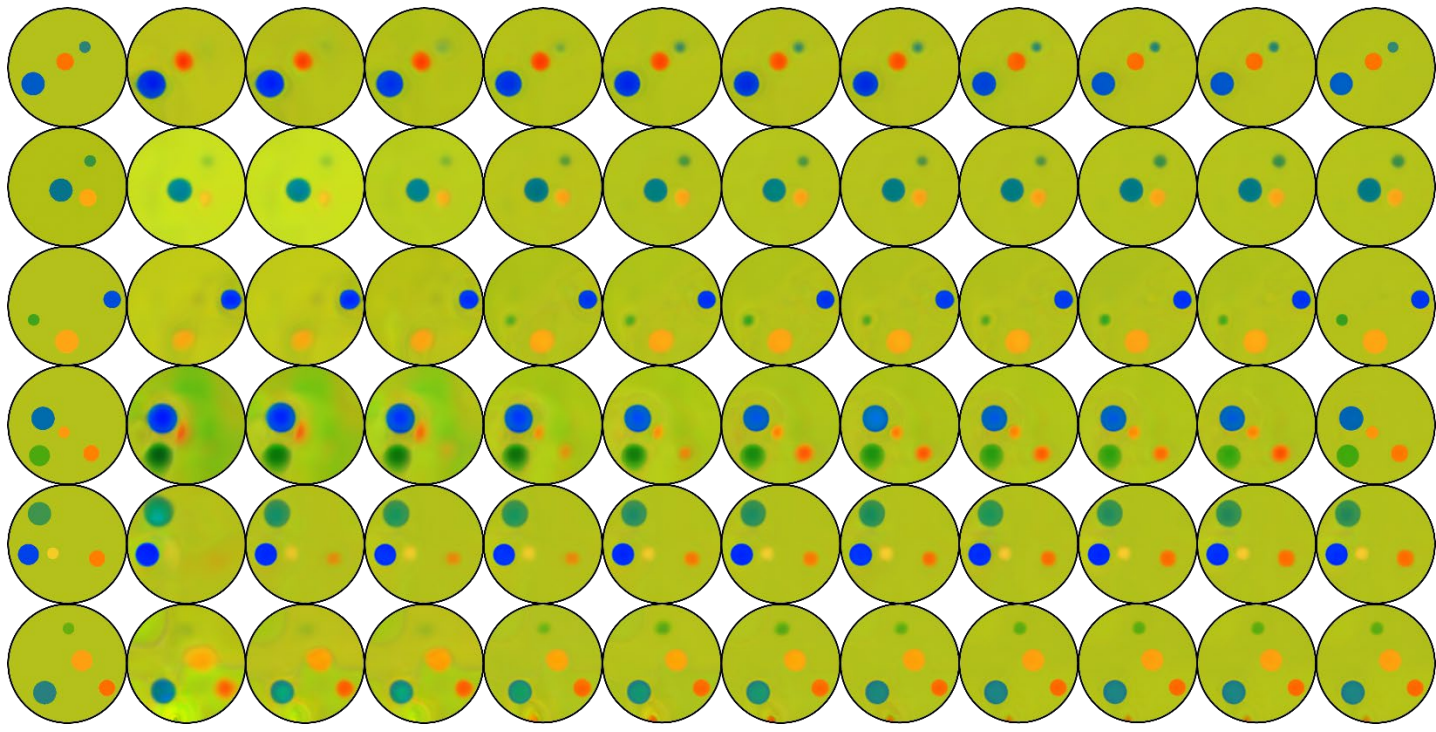


Fig. S13 The reconstruction results of **In-Distribution simulation data** (*Group of multi-phase inclusions distributions*) with the circular observation boundary. In this case, the first column is the ground truth or experimental settings, the second to fifth columns are the results based on the ***supervised image-domain reconstruction methods*** (DHU-Net, FISTA-Net, PDCISTA-Net, SWISTA-Net), the sixth to ninth columns give the results of the ***unsupervised image-domain reconstruction methods*** (DeepEIT, DiffusionEIT, ConditionDDPM and CD-EIT), the tenth to twelfth columns give the results of the ***unsupervised image-domain reconstruction methods*** (CGAN, DDPM and proposed SPfusion). These results are reconstructed by FISTA-Net.

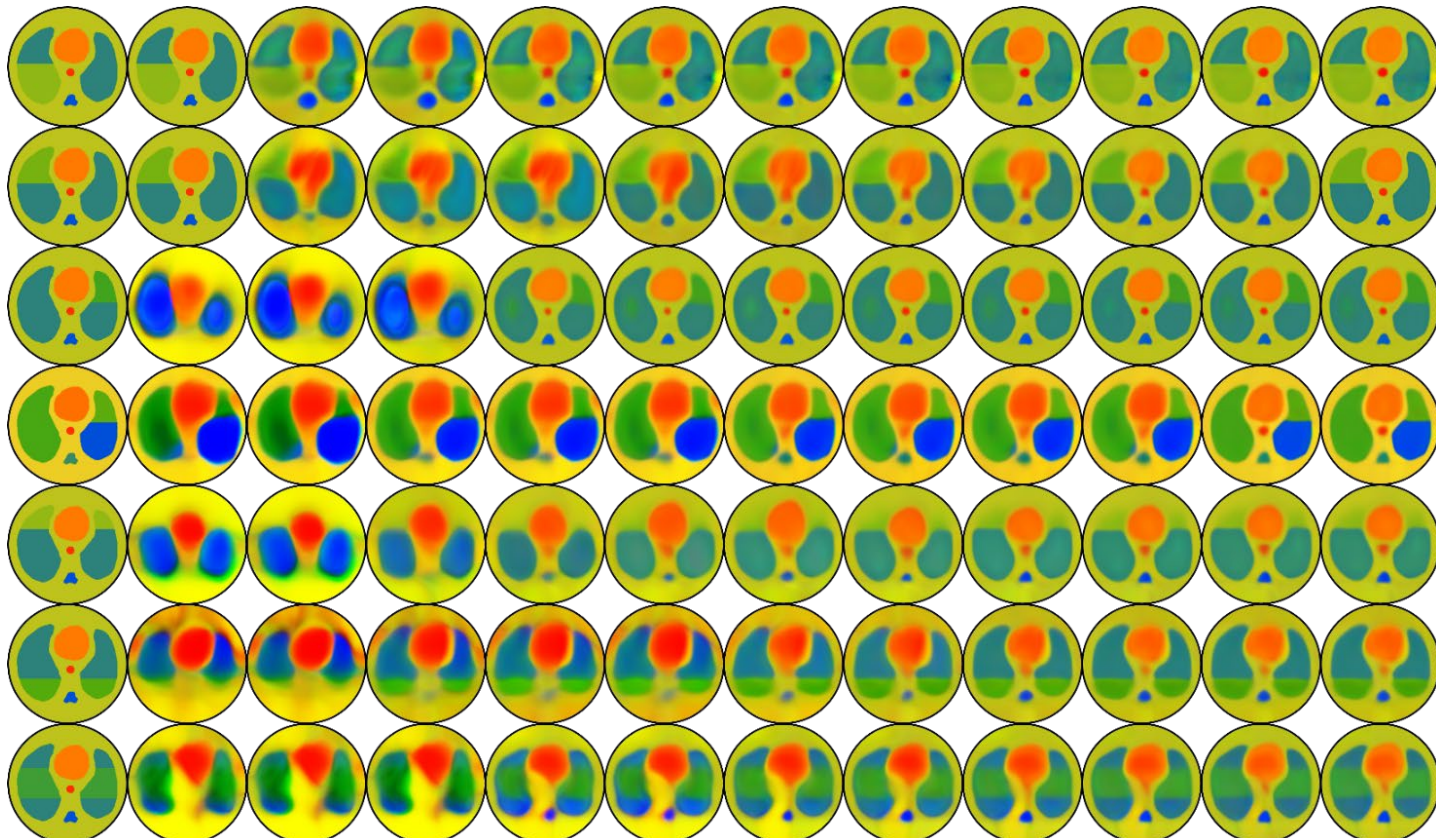


Fig. S14 The reconstruction results of **In-Distribution simulation data** (*Group of lung-shaped phantoms distributions*) with the circular observation boundary. In this case, the first column is the ground truth or experimental settings, the second to fifth columns are the results based on the ***supervised image-domain reconstruction methods*** (DHU-Net, FISTA-Net, PDCISTA-Net, SWISTA-Net), the sixth to ninth columns give the results of the ***unsupervised image-domain reconstruction methods*** (DeepEIT, DiffusionEIT, ConditionDDPM and CD-EIT), the tenth to twelfth columns give the results of the ***unsupervised image-domain reconstruction methods*** (CGAN, DDPM and proposed SPfusion). These results are reconstructed by FISTA-Net.

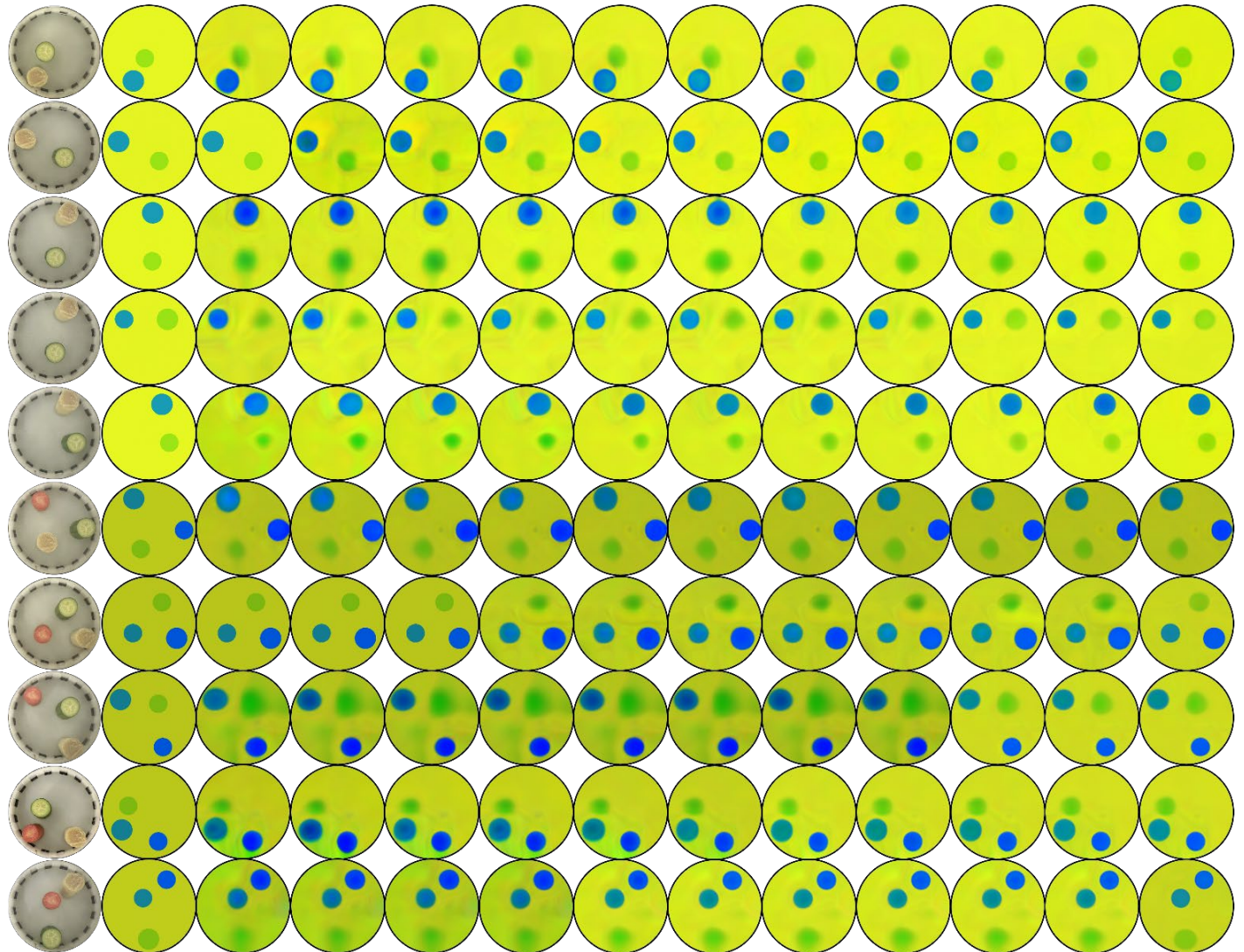


Fig. S15 The reconstruction results of **In-Distribution real-world measurement data** (*Group of multi-phase inclusions distributions*) with the circular observation boundary. In this case, the first column is the ground truth or experimental settings, the second to fifth columns are the results based on the ***supervised image-domain reconstruction methods*** (DHU-Net, FISTA-Net, PDCISTA-Net, SWISTA-Net), the sixth to ninth columns give the results of the ***unsupervised image-domain reconstruction methods*** (DeepEIT, DiffusionEIT, ConditionDDPM and CD-EIT), the tenth to twelfth columns give the results of the ***unsupervised image-domain reconstruction methods*** (CGAN, DDPM and proposed SPfusion). These results are reconstructed by FISTA-Net.

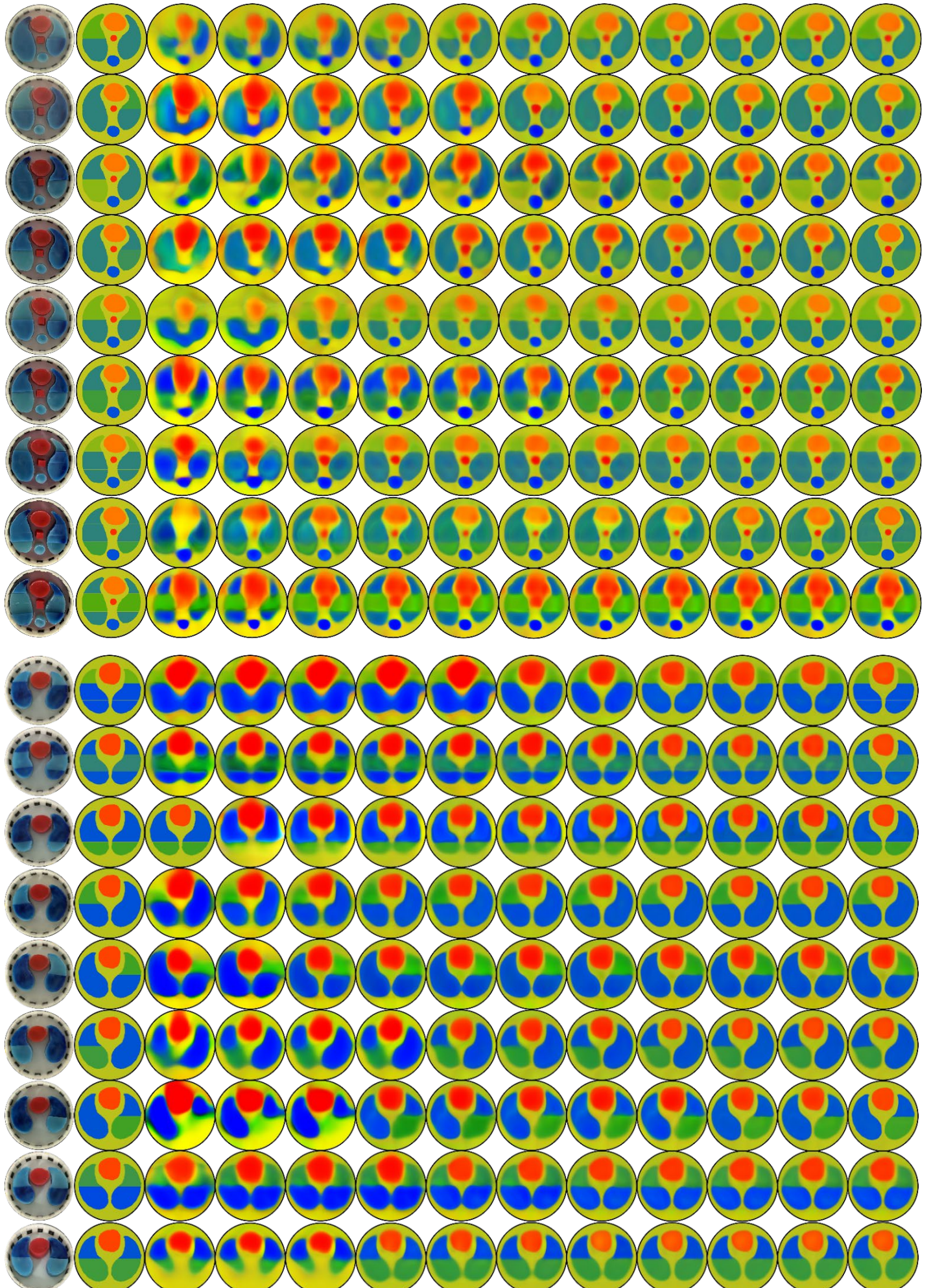


Fig. S16 The reconstruction results of **In-Distribution real-world measurement data (Group of lung-shaped phantoms distributions)** with the circular observation boundary. In this case, the first column is the ground truth or experimental settings, the second to fifth columns are the results based on the ***supervised image-domain reconstruction methods*** (DHU-Net, FISTA-Net, PDCISTA-Net, SWISTA-Net), the sixth to ninth columns give the results of the ***unsupervised image-domain reconstruction methods*** (DeepEIT, DiffusionEIT, ConditionDDPM and CD-EIT), the tenth to twelfth columns give the results of the ***unsupervised image-domain reconstruction methods*** (CGAN, DDPM and proposed SPfusion). These results are reconstructed by FISTA-Net.

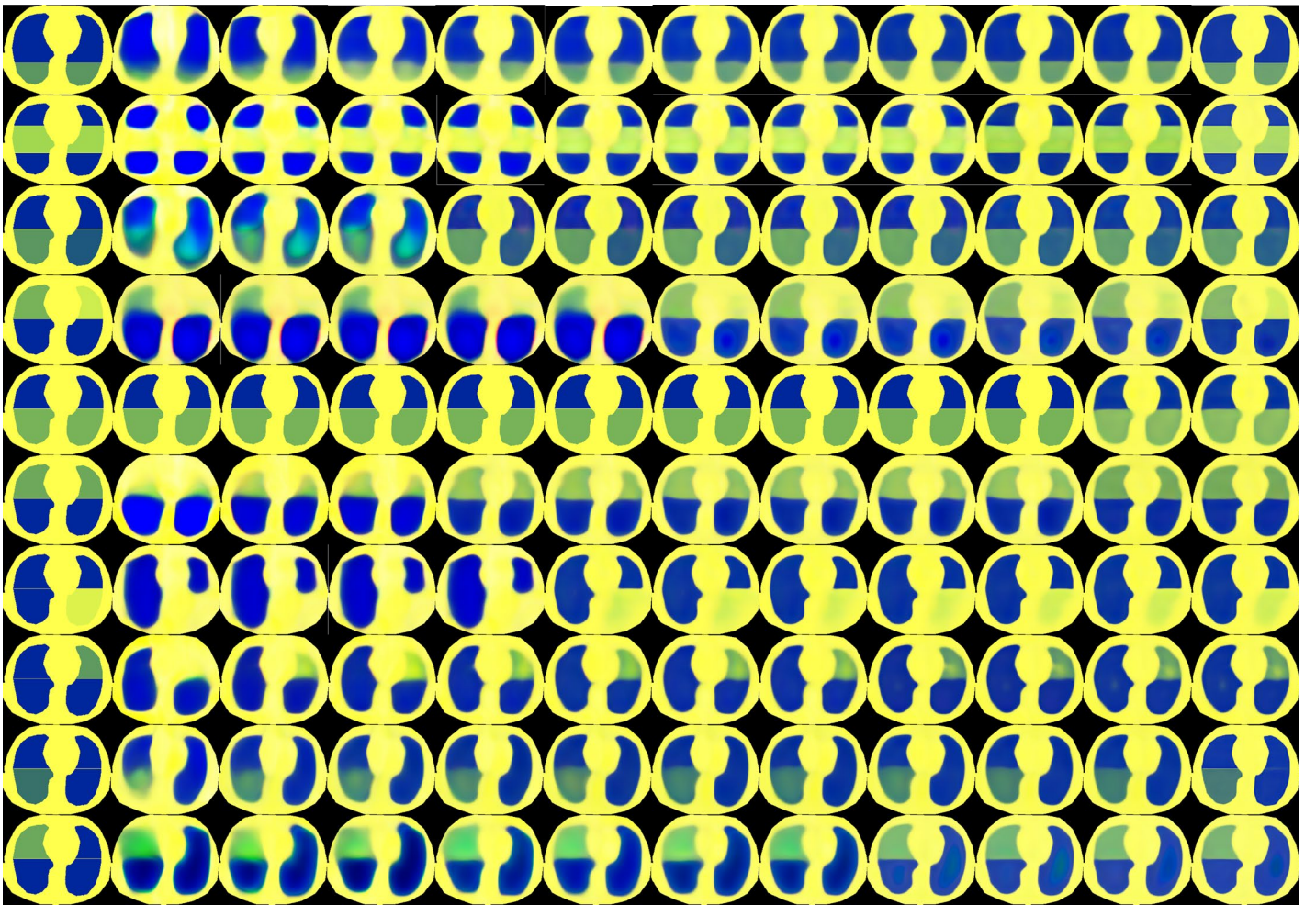


Fig. S17 The reconstruction results of Out-of-Distribution data (**Group 1**). In this case, the first column is the ground truth or experimental settings, the second to fifth columns are the results based on the ***supervised image-domain reconstruction methods*** (DHU-Net, FISTA-Net, PDCISTA-Net, SWISTA-Net), the sixth to ninth columns give the results of the ***unsupervised image-domain reconstruction methods*** (DeepEIT, DiffusionEIT, ConditionDDPM and CD-EIT), the tenth to twelfth columns give the results of the ***unsupervised image-domain reconstruction methods*** (CGAN, DDPM and proposed SPfusion). These results are reconstructed by FISTA-Net.

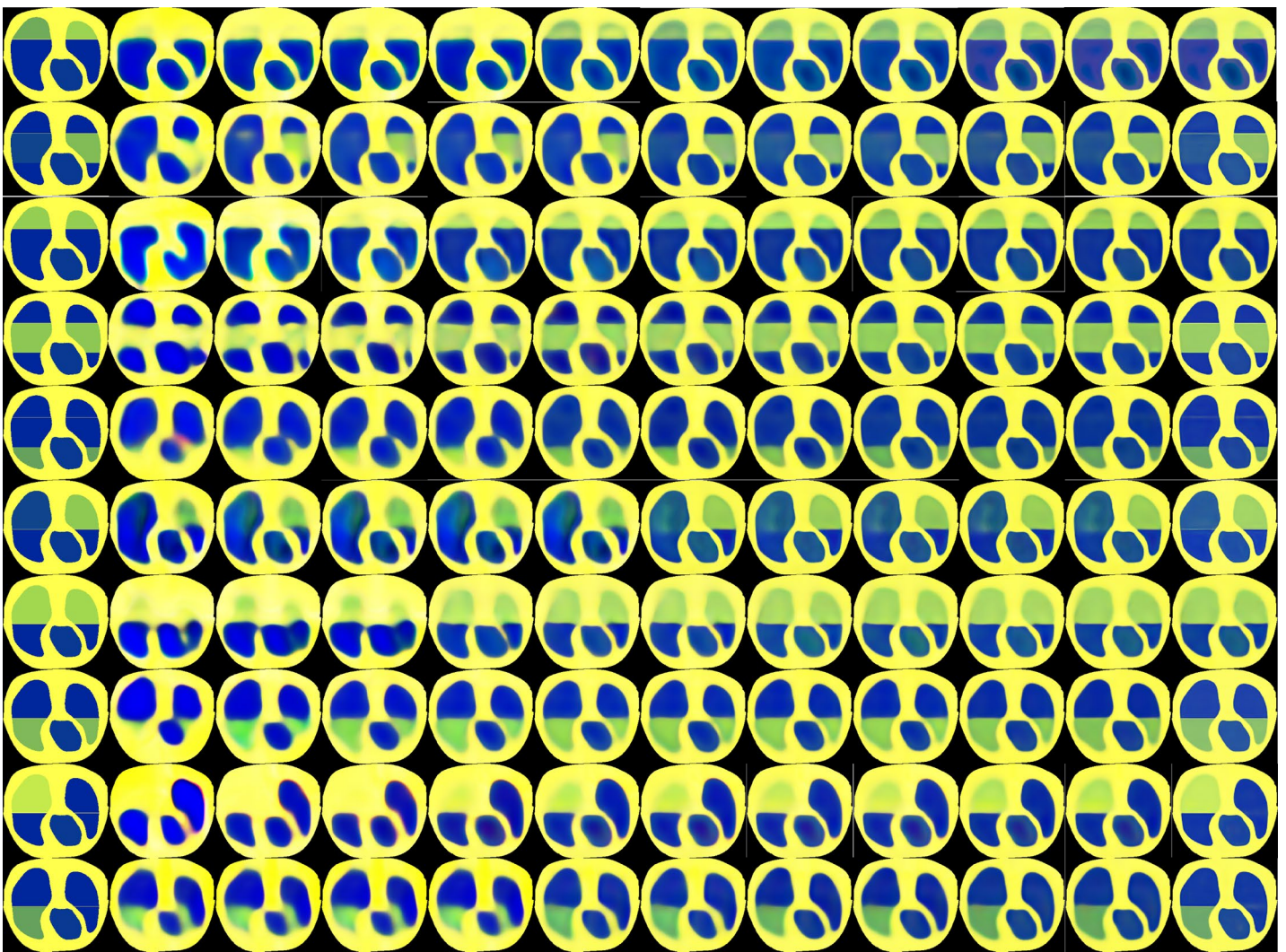


Fig. S18 The reconstruction results of Out-of-Distribution data (**Group 2**). In this case, the first column is the ground truth or experimental settings, the second to fifth columns are the results based on the ***supervised image-domain reconstruction methods*** (DHU-Net, FISTA-Net, PDCISTA-Net, SWISTA-Net), the sixth to ninth columns give the results of the ***unsupervised image-domain reconstruction methods*** (DeepEIT, DiffusionEIT, ConditionDDPM and CD-EIT), the tenth to twelfth columns give the results of the ***unsupervised image-domain reconstruction methods*** (CGAN, DDPM and proposed SPfusion). These results are reconstructed by FISTA-Net.

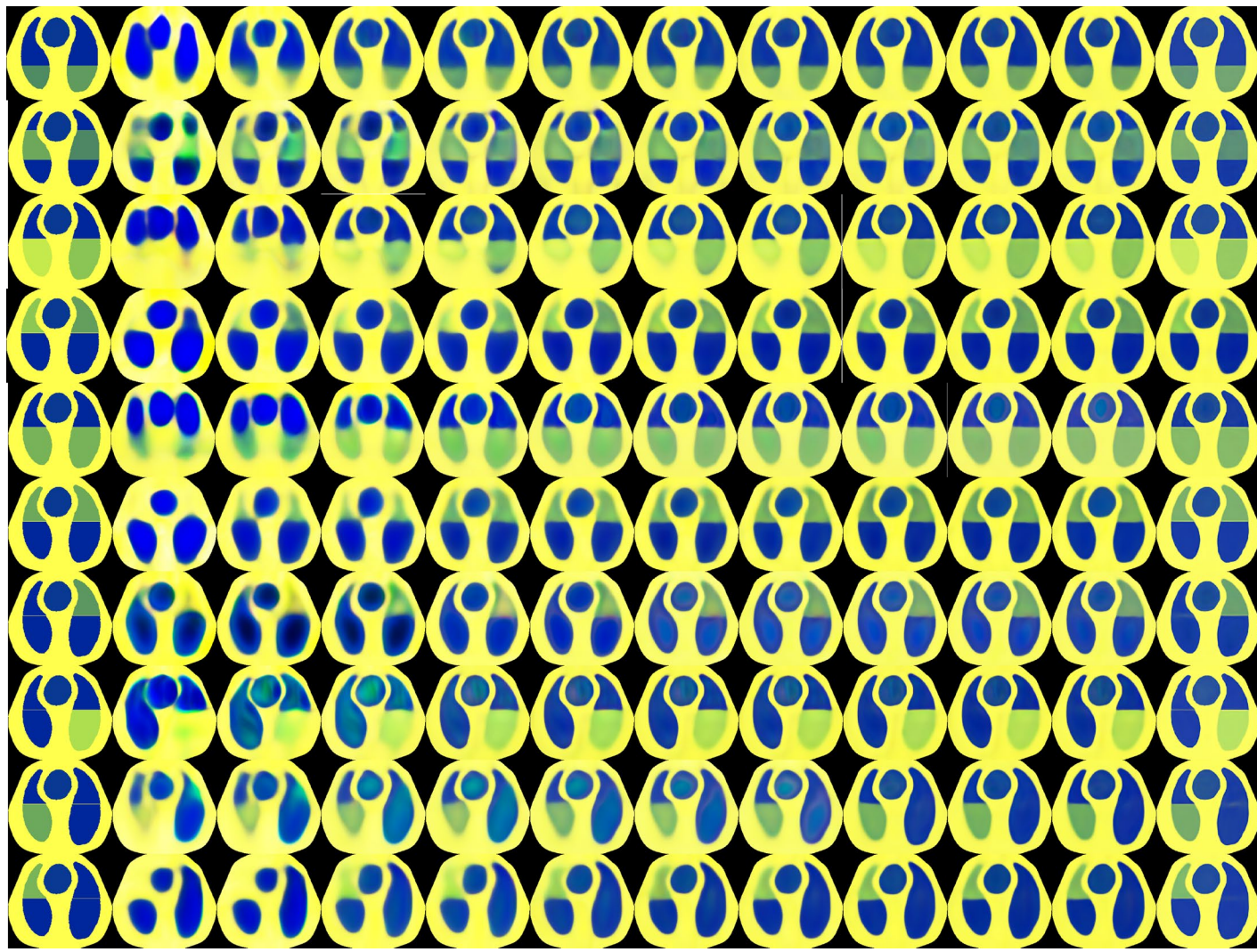


Fig. S19 The reconstruction results of Out-of-Distribution data (**Group 3**). In this case, the first column is the ground truth or experimental settings, the second to fifth columns are the results based on the ***supervised image-domain reconstruction methods*** (DHU-Net, FISTA-Net, PDCISTA-Net, SWISTA-Net), the sixth to ninth columns give the results of the ***unsupervised image-domain reconstruction methods*** (DeepEIT, DiffusionEIT, ConditionDDPM and CD-EIT), the tenth to twelfth columns give the results of the ***unsupervised image-domain reconstruction methods*** (CGAN, DDPM and proposed SPfusion). These results are reconstructed by FISTA-Net.

Table SI **In-Distribution** experiments. The average quantitative metrics (PSNR, RMSE, and SSIM) of the *real-world measurement data*.**Cases 1 to 10 corresponds to the measurement scenarios shown in Fig. S15.** The best and second-best performance are marked as red and underline, respectively.

<b>RMSE</b>	<b>CGAN</b>	<b>DeepEIT</b>	<b>DDPM</b>	<b>DHU-Net</b>	<b>FISTA-Net</b>	<b>PDCISTA-Net</b>	<b>SWISTA-Net</b>	<b>DiffusionEIT</b>	<b>Condition</b>	<b>CD-EIT</b>	<b>Ours</b>
Case 1	18.755	11.482	14.859	13.301	12.675	10.405	9.752	9.931	8.562	<u>7.896</u>	<b>6.454</b>
Case 2	20.348	19.173	14.516	13.656	12.277	10.696	9.393	8.398	7.930	<u>7.447</u>	<b>6.251</b>
Case 3	26.735	24.352	20.875	16.383	15.567	14.279	12.353	12.635	10.397	<u>9.814</u>	<b>7.928</b>
Case 4	17.526	10.633	10.251	8.135	7.794	6.591	6.089	5.945	5.158	<u>4.742</u>	<b>4.608</b>
Case 5	25.685	17.679	17.599	15.783	12.781	12.702	10.180	9.239	8.542	<u>7.687</u>	<b>6.145</b>
Case 6	18.482	16.269	15.608	14.803	13.652	12.125	11.290	10.686	9.414	<u>7.687</u>	<b>5.923</b>
Case 7	26.327	20.841	18.036	17.349	15.658	14.843	13.210	12.796	12.241	<u>11.200</u>	<b>9.617</b>
Case 8	18.071	17.049	15.036	14.159	13.636	12.227	11.032	10.877	9.391	<u>8.249</u>	<b>7.602</b>
Case 9	24.152	20.236	18.689	17.858	16.434	15.344	14.232	12.647	11.031	<u>10.069</u>	<b>8.107</b>
Case 10	24.382	22.128	20.233	19.014	18.163	17.238	16.300	15.962	14.335	<u>12.093</u>	<b>8.347</b>
<b>PSNR</b>	<b>CGAN</b>	<b>DeepEIT</b>	<b>DDPM</b>	<b>DHU-Net</b>	<b>FISTA-Net</b>	<b>PDCISTA-Net</b>	<b>SWISTA-Net</b>	<b>DiffusionEIT</b>	<b>Condition</b>	<b>CD-EIT</b>	<b>Ours</b>
Case 1	24.010	28.256	26.039	26.997	27.402	29.117	29.693	29.547	30.544	<u>31.523</u>	<b>32.054</b>
Case 2	23.416	23.932	26.380	27.933	28.056	29.842	30.499	31.454	32.618	<u>32.748</u>	<b>33.602</b>
Case 3	20.921	21.727	23.055	25.155	25.592	26.357	27.602	27.415	29.094	<u>29.609</u>	<b>31.472</b>
Case 4	24.744	29.021	29.414	31.457	31.574	33.170	33.788	33.856	34.000	<u>36.006</u>	<b>36.500</b>
Case 5	21.291	24.535	24.575	25.533	27.378	27.439	29.360	30.201	31.184	<u>32.806</u>	<b>33.772</b>
Case 6	24.094	25.194	26.520	27.439	28.494	29.753	30.178	30.507	32.240	<u>33.510</u>	<b>34.078</b>
Case 7	21.096	22.131	23.966	24.282	25.294	26.169	27.141	27.833	29.095	<u>30.231</u>	<b>32.982</b>
Case 8	23.386	23.889	24.641	25.202	26.202	27.642	28.681	28.939	30.574	<u>31.011</u>	<b>32.156</b>
Case 9	22.755	23.765	24.313	25.557	26.806	27.250	28.452	29.089	29.427	<u>30.920</u>	<b>31.998</b>
Case 10	20.411	21.898	22.340	23.267	24.126	25.191	26.758	27.753	28.736	<u>30.151</u>	<b>31.734</b>
<b>SSIM</b>	<b>CGAN</b>	<b>DeepEIT</b>	<b>DDPM</b>	<b>DHU-Net</b>	<b>FISTA-Net</b>	<b>PDCISTA-Net</b>	<b>SWISTA-Net</b>	<b>DiffusionEIT</b>	<b>Condition</b>	<b>CD-EIT</b>	<b>Ours</b>
Case 1	0.904	0.920	0.928	0.931	0.940	0.943	0.970	0.969	0.978	<u>0.973</u>	<b>0.982</b>
Case 2	0.900	0.902	0.915	0.923	0.936	0.938	0.941	0.951	0.962	<u>0.974</u>	<b>0.989</b>
Case 3	0.904	0.917	0.925	0.932	0.944	0.949	0.951	0.955	0.966	<u>0.970</u>	<b>0.979</b>
Case 4	0.908	0.918	0.922	0.936	0.947	0.950	0.962	0.964	0.970	<u>0.979</u>	<b>0.983</b>
Case 5	0.900	0.916	0.928	0.934	0.937	0.949	0.951	0.960	0.964	<u>0.972</u>	<b>0.985</b>
Case 6	0.853	0.870	0.879	0.883	0.889	0.901	0.912	0.917	0.922	<u>0.938</u>	<b>0.949</b>
Case 7	0.890	0.908	0.922	0.939	0.937	0.937	0.949	0.951	0.958	<u>0.965</u>	<b>0.974</b>
Case 8	0.883	0.897	0.910	0.913	0.922	0.939	0.940	0.954	0.968	<u>0.968</u>	<b>0.973</b>
Case 9	0.895	0.910	0.913	0.925	0.934	0.944	0.955	0.957	0.959	<u>0.961</u>	<b>0.980</b>
Case 10	0.912	0.918	0.922	0.935	0.942	0.957	0.959	0.963	0.969	<u>0.976</u>	<b>0.983</b>

Table SII **In-Distribution** experiments. The average quantitative metrics (PSNR, RMSE, and SSIM) of the *real-world measurement data*.**Cases 1 to 18 corresponds to the measurement scenarios shown in Fig. S16.** The best and second-best performance are marked as red and underline, respectively.

<b>RMSE</b>	<b>CGAN</b>	<b>DeepEIT</b>	<b>DDPM</b>	<b>DHU-Net</b>	<b>FISTA-Net</b>	<b>PDCISTA-Net</b>	<b>SWISTA-Net</b>	<b>DiffusionEIT</b>	<b>Condition</b>	<b>CD-EIT</b>	<b>Ours</b>
Case 1	30.014	21.266	21.951	17.055	18.984	15.106	14.230	10.529	9.630	<u>9.252</u>	<b>5.176</b>
Case 2	35.938	34.734	24.363	16.441	12.905	15.363	13.411	11.395	10.623	<u>10.788</u>	<b>5.777</b>
Case 3	30.557	27.643	26.352	23.912	21.535	21.348	17.975	13.797	12.821	<u>11.514</u>	<b>6.901</b>
Case 4	39.156	29.821	24.235	19.844	19.154	15.588	16.421	10.925	11.566	<u>10.492</u>	<b>5.534</b>
Case 5	28.670	25.950	21.076	16.147	16.278	14.849	13.235	10.333	10.375	<u>8.482</u>	<b>5.544</b>
Case 6	40.173	29.921	26.755	23.269	22.663	18.748	16.471	11.731	12.245	<u>10.061</u>	<b>5.963</b>
Case 7	36.809	27.766	18.096	14.492	13.704	11.949	11.051	9.772	9.396	<u>9.378</u>	<b>6.309</b>
Case 8	31.145	19.173	16.261	14.252	14.430	14.071	11.190	10.510	10.351	<u>9.757</u>	<b>7.028</b>
Case 9	32.231	29.874	21.969	18.827	15.730	14.763	13.953	12.443	11.871	<u>11.147</u>	<b>8.771</b>
Case 10	30.604	28.516	23.858	20.005	17.201	17.222	14.701	12.663	12.391	<u>10.681</u>	<b>7.746</b>
Case 11	27.079	24.953	22.178	20.624	18.797	16.650	14.377	13.233	13.481	<u>12.435</u>	<b>6.503</b>
Case 12	45.570	40.747	28.156	20.368	15.543	13.815	15.083	11.844	10.077	<u>10.201</u>	<b>5.482</b>
Case 13	36.131	26.060	19.499	14.335	15.065	12.173	12.695	9.928	8.530	<u>8.809</u>	<b>6.039</b>
Case 14	37.538	31.409	19.996	17.565	17.542	17.032	15.664	12.854	11.794	<u>12.611</u>	<b>7.969</b>
Case 15	33.537	25.239	20.316	16.960	14.575	15.266	12.911	11.589	12.443	<u>10.508</u>	<b>6.692</b>
Case 16	54.403	42.532	25.623	17.398	17.852	17.268	13.743	11.759	10.768	<u>9.654</u>	<b>6.319</b>
Case 17	27.398	24.731	19.719	17.434	17.146	13.635	12.748	10.857	9.621	<u>10.059</u>	<b>5.447</b>
Case 18	30.318	23.536	14.181	10.754	11.927	10.676	12.593	9.468	9.565	<u>9.035</u>	<b>5.879</b>
<b>PSNR</b>	<b>CGAN</b>	<b>DeepEIT</b>	<b>DDPM</b>	<b>DHU-Net</b>	<b>FISTA-Net</b>	<b>PDCISTA-Net</b>	<b>SWISTA-Net</b>	<b>DiffusionEIT</b>	<b>Condition</b>	<b>CD-EIT</b>	<b>Ours</b>
Case 1	19.909	22.949	22.644	24.848	23.901	25.900	26.420	29.007	29.817	<u>30.177</u>	<b>35.196</b>
Case 2	18.336	18.635	21.701	25.149	27.254	25.728	26.903	28.341	28.937	<u>28.812</u>	<b>34.271</b>
Case 3	19.738	20.606	21.048	21.893	22.829	22.913	24.405	26.719	27.359	<u>28.293</u>	<b>32.735</b>
Case 4	17.589	19.971	21.771	23.518	23.831	25.610	25.154	28.728	28.229	<u>29.104</u>	<b>34.630</b>
Case 5	20.311	21.168	22.978	25.307	25.229	26.042	27.055	29.193	29.168	<u>30.939</u>	<b>34.616</b>
Case 6	17.369	19.941	20.928	22.156	22.392	24.061	25.139	28.096	27.763	<u>29.473</u>	<b>33.994</b>
Case 7	18.131	20.573	24.307	26.257	26.740	27.942	28.622	29.700	30.028	<u>30.039</u>	<b>33.506</b>
Case 8	19.593	23.829	25.249	26.419	26.291	26.505	28.486	29.065	29.166	<u>29.697</u>	<b>32.543</b>
Case 9	19.288	19.963	22.636	23.979	25.536	26.071	26.575	27.538	27.941	<u>28.503</u>	<b>30.647</b>
Case 10	19.735	20.369	21.902	23.467	24.763	24.765	26.209	27.529	27.699	<u>29.004</u>	<b>31.781</b>
Case 11	20.774	21.522	22.535	23.169	24.008	25.091	26.363	27.113	26.984	<u>27.715</u>	<b>33.277</b>
Case 12	16.292	17.280	20.490	23.300	25.657	26.704	25.939	28.082	29.537	<u>29.463</u>	<b>34.797</b>
Case 13	18.282	21.134	23.682	26.406	26.035	27.850	27.534	29.680	31.108	<u>30.766</u>	<b>33.993</b>
Case 14	17.947	19.504	23.491	24.582	24.644	24.922	25.687	27.384	28.187	<u>27.608</u>	<b>31.535</b>
Case 15	18.895	21.371	23.235	24.887	26.217	25.867	27.366	28.282	27.686	<u>29.069</u>	<b>33.151</b>
Case 16	14.749	16.876	21.299	24.711	24.457	24.758	26.748	28.103	28.893	<u>29.859</u>	<b>33.550</b>
Case 17	20.723	21.620	23.578	24.644	24.794	26.788	27.368	28.752	29.775	<u>29.375</u>	<b>34.712</b>
Case 18	19.733	21.910	26.338	28.797	27.865	28.883	27.402	29.913	29.816	<u>30.334</u>	<b>34.241</b>
<b>SSIM</b>	<b>CGAN</b>	<b>DeepEIT</b>	<b>DDPM</b>	<b>DHU-Net</b>	<b>FISTA-Net</b>	<b>PDCISTA-Net</b>	<b>SWISTA-Net</b>	<b>DiffusionEIT</b>	<b>Condition</b>	<b>CD-EIT</b>	<b>Ours</b>
Case 1	0.815	0.829	0.833	0.852	0.856	0.868	0.873	0.901	0.910	<u>0.912</u>	<b>0.964</b>
Case 2	0.802	0.804	0.841	0.865	0.891	0.879	0.886	0.904	0.910	<u>0.910</u>	<b>0.963</b>
Case 3	0.814	0.826	0.831	0.844	0.847	0.851	0.865	0.886	0.895	<u>0.912</u>	<b>0.952</b>
Case 4	0.802	0.814	0.819	0.844	0.850	0.873	0.876	0.905	0.909	<u>0.914</u>	<b>0.965</b>
Case 5	0.827	0.829	0.843	0.868	0.875	0.878	0.885	0.904	0.904	<u>0.920</u>	<b>0.954</b>
Case 6	0.755	0.806	0.812	0.836	0.840	0.867	0.882	0.903	0.905	<u>0.920</u>	<b>0.963</b>
Case 7	0.788	0.821	0.855	0.873	0.872	0.887	0.895	0.905	0.910	<u>0.908</u>	<b>0.944</b>
Case 8	0.784	0.824	0.836	0.858	0.857	0.868	0.883	0.892	0.894	<u>0.900</u>	<b>0.934</b>
Case 9	0.770	0.787	0.823	0.833	0.852	0.861	0.862	0.877	0.882	<u>0.888</u>	<b>0.924</b>
Case 10	0.783	0.802	0.809	0.839	0.842	0.853	0.864	0.884	0.885	<u>0.899</u>	<b>0.947</b>
Case 11	0.810	0.819	0.828	0.839	0.844	0.859	0.869	0.877	0.876	<u>0.887</u>	<b>0.958</b>
Case 12											

Table SIII **Out-of-Distribution** experiments, where the Cases 1 to 10 are shown in Group 1, Cases 11 to 20 are shown in Group 2, and Cases 21 to 30 are shown in Group 3.The average quantitative metrics (**RMSE**) of the simulation data. The best and second-best performance are marked as red and underline, respectively.

RMSE	CGAN	DeepEIT	DDPM	DHU-Net	FISTA-Net	PDCISTA-Net	SWISTA-Net	DiffusionEIT	Condition	CD-EIT	<b>Ours</b>
Case ·1	37.556	33.274	32.593	28.604	26.206	28.120	25.215	24.934	23.361	<u>23.845</u>	<b>23.929</b>
Case ·2	47.159	34.159	35.601	33.327	27.740	28.785	27.041	28.528	27.593	<u>24.772</u>	<b>15.238</b>
Case ·3	48.524	42.247	39.368	37.295	37.066	35.135	30.446	28.037	28.622	<u>29.750</u>	<b>19.195</b>
Case ·4	39.341	30.341	25.579	21.425	20.477	22.035	19.674	19.187	17.520	<u>17.549</u>	<b>17.131</b>
Case ·5	45.130	35.060	33.395	29.575	24.828	26.481	21.404	17.944	19.615	<u>18.453</u>	<b>15.697</b>
Case ·6	45.330	34.885	33.111	28.189	29.254	25.029	25.606	19.418	16.988	<u>17.426</u>	<b>13.927</b>
Case ·7	58.401	44.654	44.086	32.248	30.154	30.393	27.616	27.484	25.365	<u>25.458</u>	<b>15.617</b>
Case ·8	39.508	30.456	38.537	18.591	17.249	18.934	18.410	19.046	17.943	<u>17.961</u>	<b>15.818</b>
Case ·9	42.165	32.285	29.534	25.428	22.946	24.827	20.543	18.470	19.362	<u>17.499</u>	<b>17.389</b>
Case ·10	41.803	41.876	36.571	35.868	28.409	28.797	26.520	30.173	22.942	<u>24.918</u>	<b>15.671</b>
Case ·11	48.138	38.953	41.929	35.368	34.314	31.711	31.449	23.107	24.684	<u>21.803</u>	<b>16.883</b>
Case ·12	40.151	39.713	39.742	27.717	25.346	24.096	28.281	23.758	22.349	<u>23.965</u>	<b>17.950</b>
Case ·13	47.972	32.895	29.596	27.452	25.902	27.384	23.999	21.756	18.142	<u>19.623</u>	<b>18.902</b>
Case ·14	42.101	41.105	28.170	27.995	26.382	24.502	21.544	24.403	20.093	<u>19.550</u>	<b>14.934</b>
Case ·15	37.898	33.458	26.105	20.520	20.292	22.400	20.432	20.697	19.410	<u>18.726</u>	<b>17.665</b>
Case ·16	53.484	46.234	42.840	34.105	36.446	36.230	29.705	25.730	22.817	<u>21.810</u>	<b>17.852</b>
Case ·17	47.933	36.332	36.481	29.895	33.064	29.054	25.775	21.818	19.730	<u>19.091</u>	<b>14.429</b>
Case ·18	58.517	48.179	40.404	29.522	31.705	27.965	24.392	22.449	19.878	<u>19.797</u>	<b>17.786</b>
Case ·19	48.893	38.220	36.288	32.030	28.143	25.923	23.872	23.068	21.508	<u>20.986</u>	<b>19.365</b>
Case ·20	44.572	39.484	33.489	30.894	28.081	23.671	23.790	22.261	23.157	<u>23.865</u>	<b>18.329</b>
Case ·21	43.929	47.047	37.838	29.864	27.518	27.574	24.379	21.234	19.307	<u>18.231</u>	<b>17.225</b>
Case ·22	51.064	43.860	38.664	38.766	33.941	32.832	33.089	20.966	21.289	<u>19.507</u>	<b>17.889</b>
Case ·23	45.754	42.325	34.752	26.024	23.986	24.938	19.586	18.701	19.301	<u>16.527</u>	<b>17.057</b>
Case ·24	40.546	42.675	32.440	34.352	32.333	31.527	29.787	26.728	24.670	<u>23.577</u>	<b>17.654</b>
Case ·25	43.670	33.008	33.893	27.535	25.889	24.199	22.070	19.705	20.455	<u>18.589</u>	<b>15.462</b>
Case ·26	43.670	33.008	33.893	27.535	25.889	24.199	22.070	19.705	20.455	<u>18.589</u>	<b>15.462</b>
Case ·27	38.811	32.541	27.014	20.981	22.349	20.630	19.063	18.525	20.025	<u>16.578</u>	<b>15.902</b>
Case ·28	54.913	40.305	32.327	27.341	23.855	23.526	20.549	15.758	15.760	<u>15.214</u>	<b>13.593</b>
Case ·29	44.584	34.695	28.668	26.804	26.034	21.987	21.595	22.045	20.094	<u>21.529</u>	<b>14.389</b>
Case ·30	55.444	40.622	28.632	28.744	25.207	23.927	22.310	21.352	21.875	<u>20.143</u>	<b>16.777</b>

Table SIV **Out-of-Distribution** experiments, where the *Cases 1 to 10* are shown in Group 1, *Cases 11 to 20* are shown in Group 2, and *Cases 21 to 30* are shown in Group 3.

The average quantitative metrics (**PSNR**) of the simulation data. The best and second-best performance are marked as red and underline, respectively.

PSNR	CGAN	DeepEIT	DDPM	DHU-Net	FISTA-Net	PDCISTA-Net	SWISTA-Net	DIffusionEIT	Condition	<u>CD-EIT</u>	<b>Ours</b>
Case ·1	17.948	18.991	19.177	20.296	21.057	20.445	21.390	21.474	22.036	<u>21.861</u>	<b>21.831</b>
Case ·2	15.948	18.745	18.388	18.960	20.537	20.233	20.769	20.299	20.594	<u>21.527</u>	<b>25.706</b>
Case ·3	15.705	16.910	17.515	17.987	18.041	18.505	19.743	20.465	20.282	<u>19.947</u>	<b>23.732</b>
Case ·4	17.551	19.809	21.285	22.802	23.189	22.558	23.541	23.755	24.542	<u>24.522</u>	<b>24.737</b>
Case ·5	16.361	18.556	18.976	20.022	21.540	20.977	22.821	24.336	23.560	<u>24.089</u>	<b>25.481</b>
Case ·6	16.335	18.617	19.068	20.472	20.143	21.508	21.306	23.694	24.842	<u>24.620</u>	<b>26.573</b>
Case ·7	14.114	16.445	16.552	19.260	19.845	19.781	20.603	20.645	21.334	<u>21.306</u>	<b>25.546</b>
Case ·8	17.499	19.747	17.703	24.010	24.662	23.845	24.098	23.800	24.310	<u>24.314</u>	<b>25.400</b>
Case ·9	16.947	19.264	20.034	21.325	22.212	21.529	23.167	24.088	23.674	<u>24.547</u>	<b>24.591</b>
Case ·10	17.021	17.001	18.172	18.340	20.360	20.239	20.953	19.836	22.208	<u>21.495</u>	<b>25.498</b>
Case ·11	15.782	17.624	16.982	18.454	18.712	19.402	19.475	22.134	21.561	<u>22.629</u>	<b>24.830</b>
Case ·12	17.361	17.455	17.448	20.571	21.340	21.778	20.391	21.896	22.429	<u>21.823</u>	<b>24.315</b>
Case ·13	15.797	19.069	19.973	20.621	21.110	20.648	21.771	22.633	24.180	<u>23.528</u>	<b>23.811</b>
Case ·14	16.957	17.169	20.434	20.484	20.992	21.621	22.726	21.652	23.331	<u>23.567</u>	<b>25.888</b>
Case ·15	17.867	18.958	21.119	23.198	23.287	22.438	23.238	23.127	23.686	<u>23.999</u>	<b>24.522</b>
Case ·16	14.871	16.137	16.800	18.773	18.195	18.254	19.969	21.203	22.244	<u>22.630</u>	<b>24.353</b>
Case ·17	15.854	18.276	18.239	19.947	19.056	20.182	21.219	22.649	23.504	<u>23.788</u>	<b>26.263</b>
Case ·18	14.098	15.795	17.323	20.047	19.421	20.507	21.684	22.393	23.449	<u>23.473</u>	<b>24.401</b>
Case ·19	15.645	17.782	18.232	19.319	20.438	21.155	21.868	22.167	22.775	<u>22.982</u>	<b>23.679</b>
Case ·20	16.474	17.531	18.955	19.638	20.472	21.938	21.900	22.473	22.124	<u>21.863</u>	<b>24.134</b>
Case ·21	16.572	15.976	17.859	19.903	20.607	20.597	21.662	22.856	23.680	<u>24.174</u>	<b>24.654</b>
Case ·22	15.270	16.587	17.674	17.651	18.800	19.087	19.018	22.961	22.843	<u>23.600</u>	<b>24.327</b>
Case ·23	16.237	16.898	18.598	21.094	21.803	21.468	23.557	23.955	23.693	<u>25.024</u>	<b>24.745</b>
Case ·24	17.274	16.833	19.210	18.707	19.233	19.441	19.928	20.867	21.557	<u>21.948</u>	<b>24.444</b>
Case ·25	16.643	19.065	18.825	20.621	21.155	21.741	22.531	23.512	23.193	<u>24.013</u>	<b>25.598</b>
Case ·26	16.643	19.065	18.825	20.621	21.155	21.741	22.531	23.512	23.193	<u>24.013</u>	<b>25.598</b>
Case ·27	17.683	19.203	20.812	23.000	22.446	23.134	23.820	24.067	23.392	<u>25.019</u>	<b>25.367</b>
Case ·28	14.649	17.325	19.235	20.684	21.849	21.974	23.142	25.441	25.435	<u>25.740</u>	<b>26.681</b>
Case ·29	16.461	18.628	20.274	20.856	21.099	22.566	22.711	22.538	23.337	<u>22.743</u>	<b>26.219</b>
Case ·30	14.568	17.264	20.294	20.254	21.393	21.836	22.444	22.823	22.615	<u>23.326</u>	<b>24.894</b>

Table SIV **Out-of-Distribution** experiments, where the *Cases 1 to 10 are shown in Group 1, Cases 11 to 20 are shown in Group 2, and Cases 21 to 30 are shown in Group 3.*The average quantitative metrics (**SSIM**) of the simulation data. The best and second-best performance are marked as red and underline, respectively.

SSIM	CGAN	DeepEIT	DDPM	DHU-Net	FISTA-Net	PDCISTA-Net	SWISTA-Net	DIffusionEIT	Condition	<u>CD-EIT</u>	<b>Ours</b>
Case ·1	0.789	0.803	0.798	0.839	0.843	0.840	0.855	0.885	0.894	<u>0.889</u>	<b>0.897</b>
Case ·2	0.795	0.830	0.824	0.836	0.858	0.855	0.865	0.855	0.865	<u>0.878</u>	<b>0.948</b>
Case ·3	0.791	0.802	0.818	0.816	0.817	0.824	0.846	0.858	0.859	<u>0.851</u>	<b>0.919</b>
Case ·4	0.814	0.845	0.869	0.905	0.908	0.902	0.915	0.918	0.926	<u>0.927</u>	<b>0.939</b>
Case ·5	0.797	0.822	0.821	0.832	0.854	0.857	0.872	0.894	0.895	<u>0.899</u>	<b>0.942</b>
Case ·6	0.793	0.832	0.827	0.847	0.846	0.870	0.871	0.899	0.908	<u>0.908</u>	<b>0.945</b>
Case ·7	0.750	0.783	0.780	0.818	0.824	0.831	0.843	0.852	0.857	<u>0.864</u>	<b>0.933</b>
Case ·8	0.767	0.813	0.792	0.906	0.912	0.905	0.906	0.907	0.915	<u>0.910</u>	<b>0.938</b>
Case ·9	0.799	0.837	0.842	0.864	0.877	0.868	0.888	0.902	0.898	<u>0.910</u>	<b>0.939</b>
Case ·10	0.776	0.780	0.820	0.815	0.837	0.842	0.850	0.832	0.866	<u>0.861</u>	<b>0.940</b>
Case ·11	0.751	0.775	0.767	0.796	0.806	0.818	0.825	0.869	0.860	<u>0.880</u>	<b>0.937</b>
Case ·12	0.805	0.801	0.801	0.847	0.855	0.864	0.851	0.878	0.888	<u>0.885</u>	<b>0.930</b>
Case ·13	0.764	0.801	0.822	0.838	0.851	0.842	0.861	0.874	0.897	<u>0.892</u>	<b>0.933</b>
Case ·14	0.790	0.800	0.831	0.836	0.841	0.857	0.875	0.869	0.891	<u>0.894</u>	<b>0.941</b>
Case ·15	0.775	0.801	0.838	0.895	0.897	0.888	0.904	0.900	0.908	<u>0.916</u>	<b>0.942</b>
Case ·16	0.726	0.757	0.763	0.798	0.793	0.793	0.823	0.851	0.875	<u>0.881</u>	<b>0.922</b>
Case ·17	0.744	0.777	0.777	0.799	0.781	0.810	0.830	0.868	0.884	<u>0.892</u>	<b>0.948</b>
Case ·18	0.707	0.751	0.778	0.821	0.811	0.830	0.851	0.865	0.880	<u>0.885</u>	<b>0.936</b>
Case ·19	0.749	0.784	0.796	0.823	0.844	0.852	0.870	0.878	0.887	<u>0.893</u>	<b>0.927</b>
Case ·20	0.781	0.813	0.836	0.840	0.846	0.866	0.871	0.883	0.883	<u>0.883</u>	<b>0.938</b>
Case ·21	0.775	0.769	0.799	0.836	0.844	0.846	0.864	0.888	0.900	<u>0.909</u>	<b>0.936</b>
Case ·22	0.757	0.775	0.798	0.799	0.817	0.828	0.824	0.891	0.888	<u>0.897</u>	<b>0.930</b>
Case ·23	0.773	0.758	0.802	0.861	0.874	0.869	0.902	0.908	0.905	<u>0.923</u>	<b>0.943</b>
Case ·24	0.781	0.747	0.808	0.814	0.818	0.844	0.852	0.873	0.884	<u>0.892</u>	<b>0.934</b>
Case ·25	0.784	0.797	0.806	0.825	0.842	0.847	0.863	0.881	0.880	<u>0.893</u>	<b>0.945</b>
Case ·26	0.784	0.797	0.806	0.825	0.842	0.847	0.863	0.881	0.880	<u>0.893</u>	<b>0.945</b>
Case ·27	0.796	0.811	0.839	0.867	0.864	0.877	0.886	0.896	0.895	<u>0.909</u>	<b>0.945</b>
Case ·28	0.759	0.792	0.834	0.847	0.867	0.872	0.884	0.917	0.914	<u>0.919</u>	<b>0.948</b>
Case ·29	0.760	0.799	0.836	0.841	0.848	0.874	0.884	0.887	0.894	<u>0.881</u>	<b>0.952</b>
Case ·30	0.734	0.780	0.838	0.842	0.859	0.865	0.881	0.888	0.887	<u>0.899</u>	<b>0.948</b>